DOCUMENTED BRIEFING

RAND

Rapid Force Projection Technologies

Assessing the Performance of Advanced Ground Sensors

John Matsumura, Randall Steeb, Randall G. Bowdish, Scot Eisenhard, Gail Halverson, Thomas Herbert, Mark Lees, John D. Pinder

Prepared for the
United States Army
Office of the Secretary of Defense

Arroyo Center
National Defense Research Institute

Approved for public release; distribution unlimited

PREFACE

This documented briefing summarizes the research emerging from an ongoing RAND project that has been supporting the Rapid Force Protection Initiative (RFPI) Advanced Concept Technology Demonstration (ACTD). This project was jointly sponsored by the Office of the Assistant Secretary of the Army for Research, Development, and Acquisition and the Office of the Under Secretary of Defense (Acquisition and Technology) with the goal of exploring new technology concepts for the ACTD. The focus of this year's research was on advanced ground sensors—specifically the air-deliverable acoustic sensor (ADAS)—with emphasis on how such sensors might fit into the current RFPI hunter–standoff killer concept. High-resolution simulation was used to examine and quantify many of the key aspects of performance, environmental effects, and military utility. This work has been shared with those involved in the ACTD, including the RFPI ACTD program offices. This work should be of interest to defense policymakers, acquisition executives, concept developers, and technologists.

The research was conducted in the Force Development and Technology Program of RAND's Arroyo Center and the Acquisition Technology Policy Center of RAND's National Defense Research Institute (NDRI). Both the Arroyo Center and NDRI are federally funded research and development centers, the first sponsored by the United States Army and the second sponsored by the Office of the Secretary of Defense, the Joint Staff, the unified commands, and the defense agencies.

CONTENTS

Preface iii
Summary vii
Abbreviations xiii

1. INTRODUCTION 1
2. SCENARIO 5
3. METHODOLOGY 10
4. INITIAL RESULTS 15
5. OBSERVATIONS 38

Appendix: ADVANCED ACOUSTIC SENSOR MODEL 41

Bibliography 65

SUMMARY

EXPLORING NEW TECHNOLOGY CONCEPTS

Over the past several years, RAND has been exploring how new concepts made viable with emerging technologies can dramatically improve the effectiveness of light ground forces, particularly in the early-entry role. Motivation for this area of research is derived from studies showing that the U.S. military will need to deploy with greater speed, lethality, and survivability in the future, and that light forces will be the first deployed.

Limitations of recent capability were observed during the Desert Shield build-up, where airborne ground forces such as the 82nd Division Ready Brigade (DRB) were deployed to secure key terrain without a credible anti-armor capability.[1] Such improvements to early-entry capabilities appear even more germane in light of the concomitant reductions in prepositioned forces abroad *and* the rapid increase in threat uncertainty. *Thus, as difficult as the early-entry challenge has been in the recent past, early signposts suggest even more difficult challenges ahead.*

One key concept that has received much attention within the RFPI ACTD is the *hunter–standoff killer* concept. Recent RAND research[2] has shown that this concept has the potential to revolutionize light force operations through the use of maturing technologies. By using advanced

---

[1]Although USAF ground-attack aircraft arrived into the Kuwaiti theater of operations (KTO) rapidly, their complement of munitions did not arrive until much later. The 82nd DRB was equipped with HMMWVs with TOW missiles and light tanks, but these short-range, lightly armored, direct fire systems are not intended to carry out a prolonged defense against massed heavy forces. Looking to the future, more efficient prepositioned munitions may help to alter this and *ideally* may do so on the margin; however, these anti-armor capabilities will still be limited by the threat (e.g., air defense network, countermeasures, tactics, etc.), the environment (e.g., prevailing weather conditions, availability of air basing, etc.), and many other conditions.

[2]See Randall Steeb and John Matsumura et al., *Rapid Force Projection: Exploring New Technology Concepts for Light Airborne Forces*, Santa Monica, CA: RAND, DB-168-A/OSD, 1996, and Randall Steeb and John Matsumura et al., *Rapid Force Projection Technologies: A Quick-Look Analysis of Advanced Light Indirect Fire Systems*, Santa Monica, CA: RAND, DB-169-A/OSD, 1996.

reconnaissance, surveillance, and target acquisition systems (RSTA) as "hunters" and emerging precision-guided weaponry as "standoff killers," light forces can dramatically improve both their lethality and survivability. Essentially, the successful application of the hunter–standoff killer concept allows a shaping of the battle in the extended-close area and results in a dramatically reduced-intensity close fight.

DISTRIBUTED SENSOR NETWORKS AS HUNTERS ON THE BATTLEFIELD

The U.S. Army is exploring ways to leverage sensor and information technologies for improving the future battlefield. Among the many technologies being explored by the Rapid Force Projection Initiative (RFPI) Advanced Concept Technology Demonstration (ACTD) is an innovative new distributed sensor system called the air-deliverable acoustic sensor (ADAS). Unlike the remotely monitored battlefield sensor system (REMBASS) used in the Vietnam War, which could be used to detect the presence of enemy vehicles at predetermined locations, ADAS can locate, track, and, to some extent, classify enemy vehicles over large areas by detecting and recognizing their acoustic signatures.[3]

Because these sensors use acoustic waves, their performance can be much less sensitive to line-of-sight (LOS) restrictions than that of the imaging sensors being evaluated in the RFPI ACTD.[4] This can be a significant advantage in certain types of terrain because the sensors can maintain area coverage yet not be exposed. Also, because ADAS units are relatively small and lightweight, they can be air delivered or hand emplaced in areas that might be considered high risk for a manned forward observer.

At the request of the U.S. Army and USD(A&T), RAND's Arroyo Center and National Defense Research Institute are assessing the utility of the

[3]Ultimately, groups of ADAS would be deployed as part of a distributed network of sensors and communication nodes that can cover relatively large areas on the battlefield.

[4]The ability of an acoustic ground sensor to operate without LOS is largely dictated by wind speed and direction, and the temperature gradient near the surface. Non-LOS performance is enhanced greatly by positive temperature gradients, which are most common at night. Also, because wind speed increases with altitude, acoustic sensor performance is enhanced toward the wind and degraded away from it.

ADAS system in its envisioned role as one of the key hunter systems in the hunter–standoff killer concept. Although there are several hunters planned for the ACTD, ADAS is unique among the other RFPI sensors in that it is not an imaging sensor. Further, there is very little operational data available to support its application in a battlefield context. Thus, one of the key underlying goals of our research effort this year is to help establish guidelines for developing appropriate tactics, techniques, and procedures (TTPs) for networks of advanced acoustic sensors like ADAS.

STRENGTHS AND WEAKNESSES OF THE ADAS NETWORK

Three key questions were posed as part of the research process. They were intended to assess the utility of ADAS based on its specific characteristics and its physical and environmental limitations at the force-on-force level. The three specific research questions will be asked and answered in the following subsections.

Question 1: How does ADAS generally contribute to force performance?

Our analysis showed that the ADAS network serving as a hunter has the potential to provide information at many levels, including broad situational awareness, cueing for other RSTA assets, and even detailed targeting information for weapon systems. The network can do a good job of covering large areas; however, its coverage is generally incomplete and imprecise.[5] In conjunction with this, we also found that, like most other battlefield sensors, ADAS performance is largely dictated by the environmental conditions in which it operates.

The key advantages of ADAS over other more conventional sensors include (1) its ability to be rapidly emplaced, (2) its relatively stealthy presence once deployed, (3) its ability to cover areas beyond LOS, and

[5]Unlike imaging sensors, which have a relatively constant probability of detection, acoustic sensors generally detect only a subset of the targets, and the subset varies with time depending on noise levels, degree of target clustering, number of microphones sensing the targets, environmental conditions, and other factors. Further, target location errors can be significant. These factors are discussed in detail in the "Initial Results" section of the main text.

(4) its relatively low levels of required maintenance. These factors were especially important because, in the scenario used for the analysis, there were many dismounted enemy infantry operating in the area where the ADAS network was emplaced.

Question 2: What are the key limitations of ADAS and how can they be overcome?

Our analysis revealed two key limitations of ADAS: (1) difficulties in acquiring targets—too many targets are missed, and (2) unexpectedly large location errors for those targets that are acquired.

When emplaced in the numbers and density defined by representatives of the Dismounted Battlespace Battle Laboratory (DBBL), the coverage provided by the ADAS network was usually incomplete, resulting in a severe understatement of the actual threat present.[6] ADAS could be used in conjunction with imaging sensors to detect and confirm the presence of potential threats. Using ADAS alone, however, it was difficult to determine the number of targets present and, therefore, difficult to gauge the correct level of response for fires. Further, the system becomes easily saturated by high densities of loud vehicles, which results in an underestimation of target density. The high density of loud targets also serves to increase the noise level, which reduces the effective range of target acquisition.

The second limitation of ADAS that was apparent in our analysis involves target location accuracy. While an ADAS network can provide fairly accurate location estimates, particularly when the targets are close to the sensors and the geometry is favorable, more distant location estimates are generally less accurate because of poor geometry and large bearing errors (due to low signal-to-noise ratios). In some cases, bearing lines were even matched incorrectly, resulting in ghost targets with very large location errors.[7]

The lack of completeness and lower-than-expected accuracy of the ADAS networks were both a strong function of the "baseline" emplacement pattern. We

---

[6]It was not unusual for an order-of-magnitude underestimation to occur.

[7]This occurs, for example, when bearing lines of targets determined to be similar by the network (e.g., two T-72s) are mistaken for the same target and fused, resulting in an erroneous triangulation.

found, however, that both of these limitations could be mitigated by adding more sensors and modifying the laydown.

Question 3: How might ADAS best be used with other RFPI systems?

We are still actively researching the answer to this third question, which tends to be an open-ended one because the RFPI systems, their capabilities and possible applications, are all still evolving. Nonetheless, initial analysis suggests that acoustic sensors are a very good match with large-footprint weapons such as the enhanced fiber optic guided missile (EFOG-M). While the ADAS networks did not provide the degree of location accuracy requested by DBBL, the footprint of the EFOG-M system was large enough to compensate for the larger targeting errors. It was also apparent that such networks could be used to cover "null" spaces on the battlefield. Because of its low profile, enduring presence, minimal maintenance, and potentially large areas of coverage, ADAS appears to be a natural system for monitoring plausible, but less likely, enemy avenues of approach in economy-of-force missions.

OBSERVATIONS

Based on our analysis this year, we see networks of advanced acoustic sensors like ADAS providing information across a broad operational spectrum, from high-level situational awareness down to detailed targeting information. Nonetheless, we emphasize that these sensors come with unique, inherent limitations. Perhaps most critically, such sensors can become saturated fairly easily, resulting in an incomplete representation of the target set. This limitation can, however, be overcome by increasing the number and density of sensors in the network, and by using them in conjunction with other sensors, as is often a preferred military solution.

While many issues still need to be resolved, future work should focus on assessing ADAS as part of the RFPI system-of-systems. Questions about how best to integrate ADAS with other RSTA systems and organize the force accordingly also need to be addressed. We are taking steps in this direction and hope to provide more insights in the near future.

ABBREVIATIONS

ACTD	Advanced Concept Technology Demonstration
ADAS	Air Deliverable Acoustic Sensor
AOS	Advanced Overwatch Sensor
ARDEC	Armaments Research, Development, and Engineering Center
ARL	Army Research Laboratory
ASP	Acoustic Sensor Program
CAGIS	Cartographic Analysis and Geographic Information System
DBBL	Dismounted Battlespace Battle Lab
DFAD	Digital Feature Attribute Data
DRB	Division Ready Brigade
DTED	Digital Terrain Elevation Data
EFOG-M	Enhanced Fiber Optic Guided Missile
FAE	Fuel Air Explosives
FLIR	Forward Looking Infrared
FO	Forward Observer
GREN	Grenadier
HRS	High-Resolution Scenario
IMF	Intelligent Minefield
LOS	Line of Sight
MADAM	Model to Assess Damage to Armor with Munitions
NEA	Northeast Asia

NK	North Korea
REMBASS	Remotely Monitored Battlefield Sensor System
RFPI	Rapid Force Projection Initiative
RJARS	RAND's Jamming Aircraft and Radar Simulation
RM	Rifleman
RSTA	Reconnaissance, Surveillance, and Target Acquisition
RTAM	RAND's Target Acquisition Model
SAW	Squad Automatic Weapon
SEMINT	Seamless Model Interface
TLE	Target Location Error
TRAC	TRADOC Analysis Center
TRADOC	Training and Doctrine Command
TTP	Tactics, Techniques, and Procedures
WAM	Wide Area Munition

1. Introduction

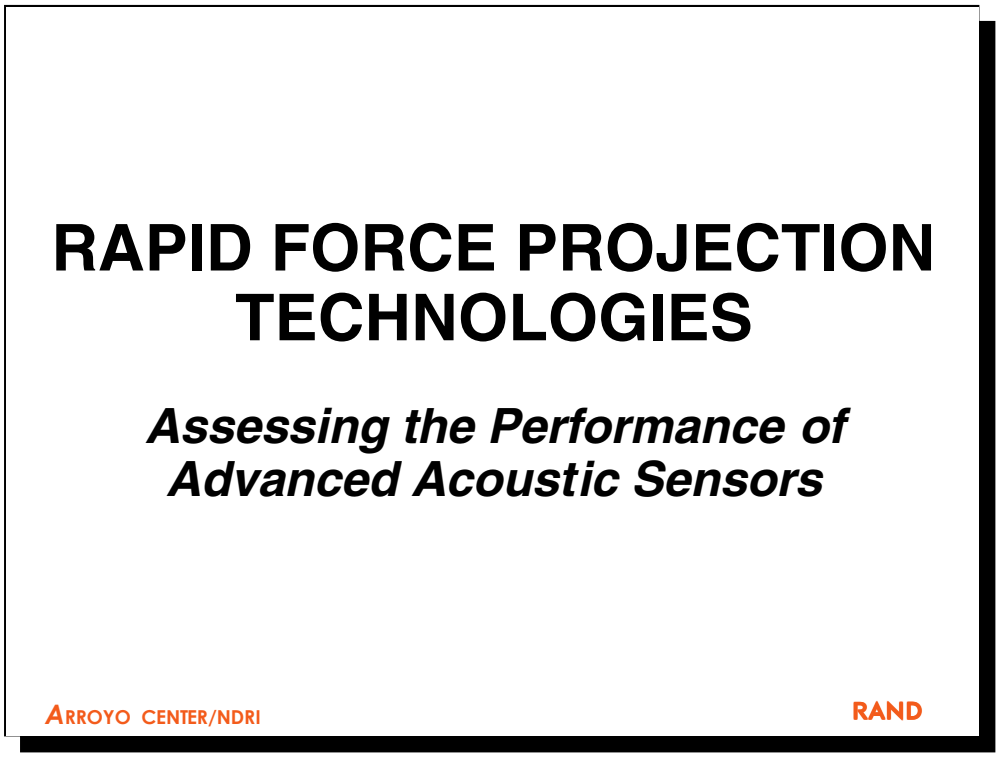

This documented briefing provides an interim report on research that was conducted for the Rapid Force Projection Technologies (RFPT) project at RAND. The focus of this year's research was on the advanced ground sensors, with particular emphasis on the air-deliverable acoustic sensor (ADAS).[1] Since advanced acoustic sensors like the ADAS are relatively new to the military, our primary intent this year is to help soldiers/users understand the utility and limitations of such sensors relative to the more commonplace imaging sensors.

The RFPT project is an ongoing effort that has supported the Rapid Force Projection Initiative (RFPI) Advanced Concept Technology Demonstration (ACTD) since its inception. The overall intent of this project has been to examine new concepts in conjunction with enabling technologies for improving light force capabilities. This research is sponsored by the Office of the Assistant Secretary of the Army for Acquisition, Logistics, and Technology and the Office of the Under Secretary of Defense (Acquisition and Technology), and it is jointly managed at RAND through two federally funded research and development centers (FFRDCs), the Arroyo Center and the National Defense Research Institute.

---

[1]ADAS is a 5-microphone sensor system being built by Textron Systems Corporation. A description of the system and its characteristics can be found in J. D. Pinder and J. Matsumura, "Ground-Based Acoustic Sensor Networks: An Analysis of Military Utility Based on Modeling and Simulation," Third NATO-IRIS Joint Symposium: Innovation in Military and Security Sensing, *Proceedings*, Quebec City, Canada: October 19–23, 1998 (forthcoming).

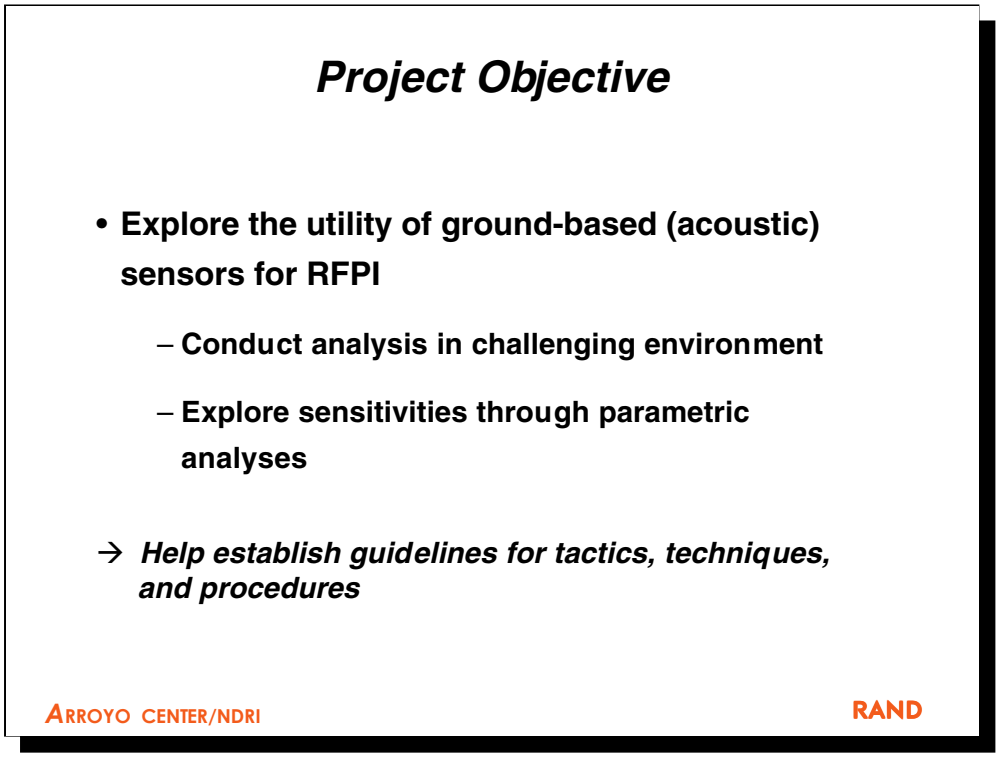

The specific objective of this year's research was to examine the ADAS system, as part of the "system-of-systems" associated with the ACTD. ADAS is used as a surrogate for the generic class of advanced acoustic ground-based sensors that might be used with future light forces. Representatives of the users at the Dismounted Battlespace Battle Lab asked that our analysis be conducted for a stressful environment, involving close terrain. Additionally, because of the uncertainty associated with the environment in which these sensors would operate (e.g., weather, noise, etc.), we parametrically adjusted variable conditions related to weather and noise in our simulation.

The ADAS system is planned to be one of the key *hunter* systems in the *hunter–standoff killer* concept that will be examined in the ACTD. Although there are several "hunters" planned for the ACTD, ADAS is unique among the other RFPI sensors in that (1) it is not an imaging sensor and (2) there is very little operational data to support its application in a battlefield context. Thus, one of the key underlying goals of our research effort this year is to help establish guidelines for developing appropriate tactics, techniques, and procedures (TTPs) for ADAS (that are also applicable to other advanced acoustic sensors).

Research Questions

- **How do acoustic sensors generally contribute to force performance?**
- **What are the key limitations of acoustic sensors and how can they be overcome?**
- **How might acoustic sensors best be used in conjunction with other RFPI systems?**

ARROYO CENTER/NDRI RAND

The three questions that were posed as part of the research process are shown above. Basically, they are designed to assess ADAS along the following lines: sensor design and functional characteristics, physical and environmental limitations, and potential for contribution to military utility at the force-on-force level.

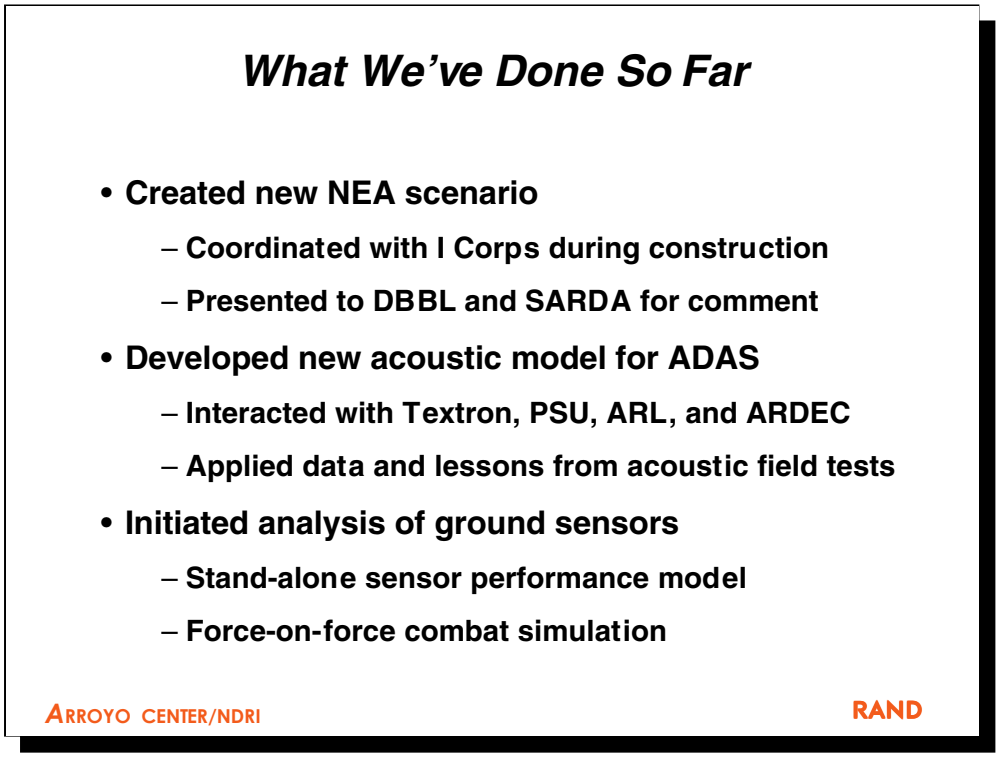

At the time of this document's publication, there have been three major areas of accomplishment. First, we completed the development of a new Northeast Asian (NEA) scenario. This scenario is based on TRAC's high-resolution scenario (HRS) 43 and, to a lesser extent, HRS 41. Second, we designed and developed a new acoustic sensor model to capture the phenomenology of the battlefield and represent the performance of an ADAS network.[2] This model was developed with input from Textron, Penn State University, the U.S. Army Research Lab (ARL), and the U.S. Army Armaments Research, Development, and Engineering Center (ARDEC). Data, observations, and insights from a series of recent field tests were also incorporated where appropriate. Our third and most recent accomplishment was to perform an initial evaluation of the ADAS system, in terms of both individual sensor and network performance, and overall force-on-force utility.

[2]We had developed an earlier acoustic sensor model to represent the advanced overwatch sensor (AOS), built by Alliant-Techsystems. A new model had to be developed for ADAS, which was designed by Textron Systems Corporation, because it is significantly different in terms of its functionality and characteristics.

2. Scenario

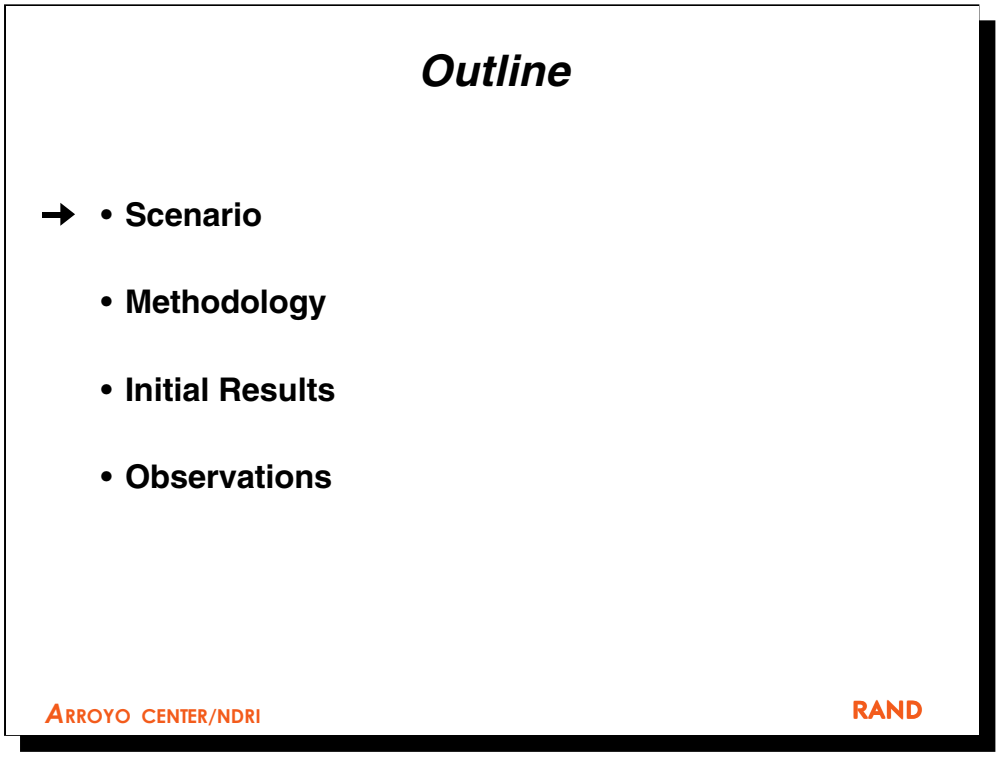

This report is divided into four major sections. We start by defining, in limited detail, the scenario that we used for this year's analysis.

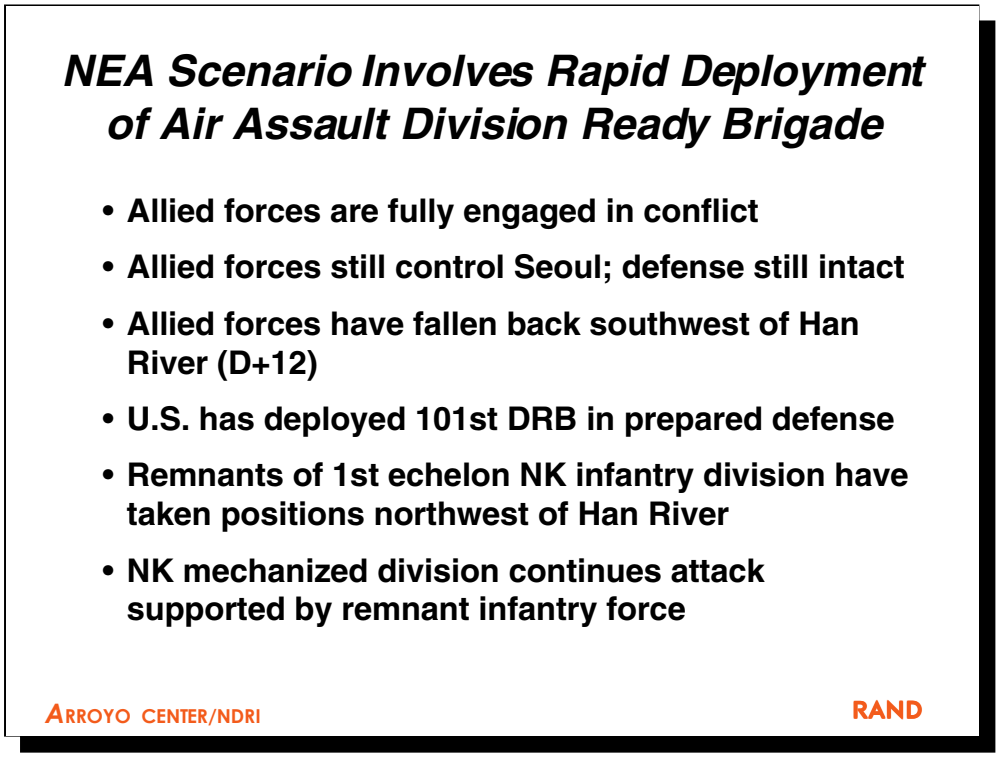

Although the emphasis for the RFPI ACTD tends to be on early-entry operations, force projection *capabilities* can also be appropriate for other phases of battle. For example, the highly fluid NEA environment may require very rapid in-country mobility coupled with high levels of lethality to counter an overwhelming attack by a large mechanized infantry force. U.S. units equipped with RFPI capabilities would be, in principle, ideal for creating a defense against such attacks. The NEA scenario, pitting a DRB light force in defense against an overmatching attacking heavy force, is representative of a class of early-entry operations, and it appeared to provide a suitable framework for exploring many of the key questions that define our study.

As indicated earlier, the scenario we used for this analysis is based on TRAC HRS 43 and 41. The timing of this scenario is such that the U.S. and allied forces are already fully engaged in conflict. Although the enemy has successfully penetrated as far as the Han River in some areas, the allied forces are still in control of Seoul. As part of its responsive defense, the United States deploys the 101st Division Ready Brigade (DRB) to protect two key river crossings along the Han. NK infantry forces are already positioned on the north side of the Han (remnants from an earlier battle, in which the allied force withdrew). NK commits a mechanized division to join with the dismounted infantry already in place for a combined forces attack across the river.

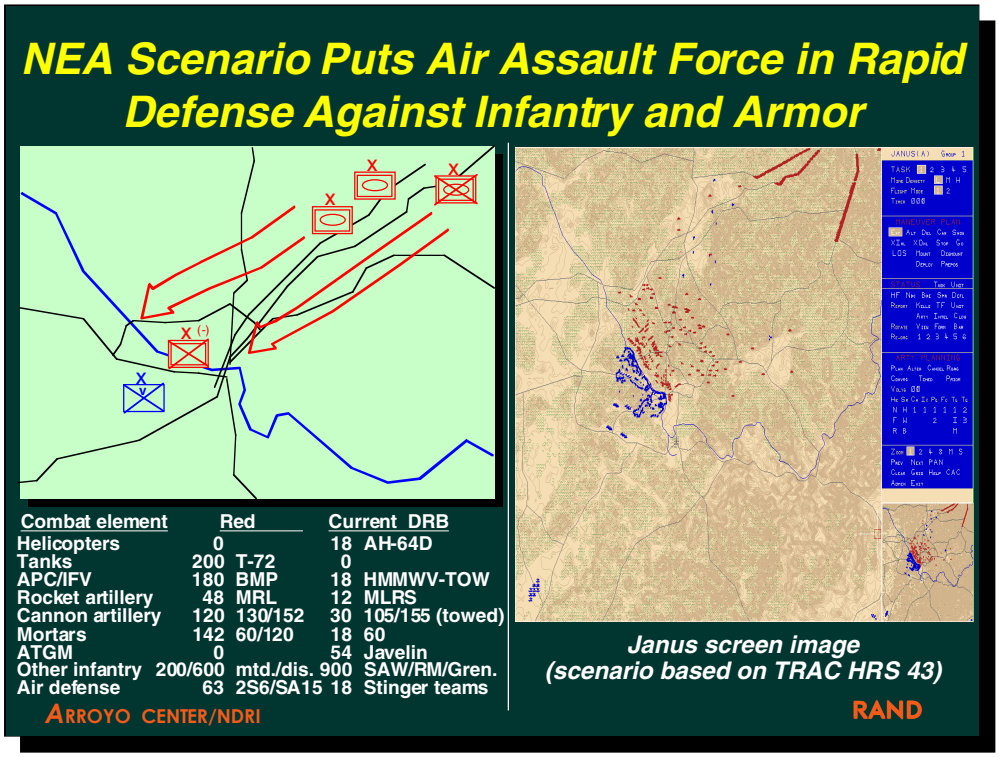

A schematic of the scenario just described is shown above, along with a screen image of the simulation.[3] In both cases, the images correspond to the starting point of our scenario. The NK mechanized infantry is beginning its movement along the few main roads available. The NK dismounted infantry is deployed north of the Han, awaiting the arrival of the mechanized forces for a combined forces attack. Although it is not evident from the images, the NK forces also have considerable numbers of artillery tubes and cannons that support the river crossing. Thus, the threat the 101st DRB must defend against is a triangular one, consisting of dismounted infantry, armored combat vehicles, and long-range artillery. The composition of this threat is that of a typical Russian mechanized regiment, as might be found in many different countries.

The DRB begins its defense with a deep attack. Forward observers (FOs) positioned deep in enemy territory provide cueing and targeting information to Apache attack helicopters equipped with millimeter-wave (MMW) Hellfire anti-tank missiles. This helps to "shape" the NK mechanized infantry force. As the mechanized force closes to the Han, the DRB relies on its other organic assets, artillery and direct fire weapons, to hold the defense. Although the DRB may have a considerable advantage in position—defending a river crossing—it is clear from the force ratios shown above that the DRB is also greatly outnumbered.

[3]Janus is a high-resolution, force-on-force combat simulation that was used for evaluating "system-of-systems" performance levels.

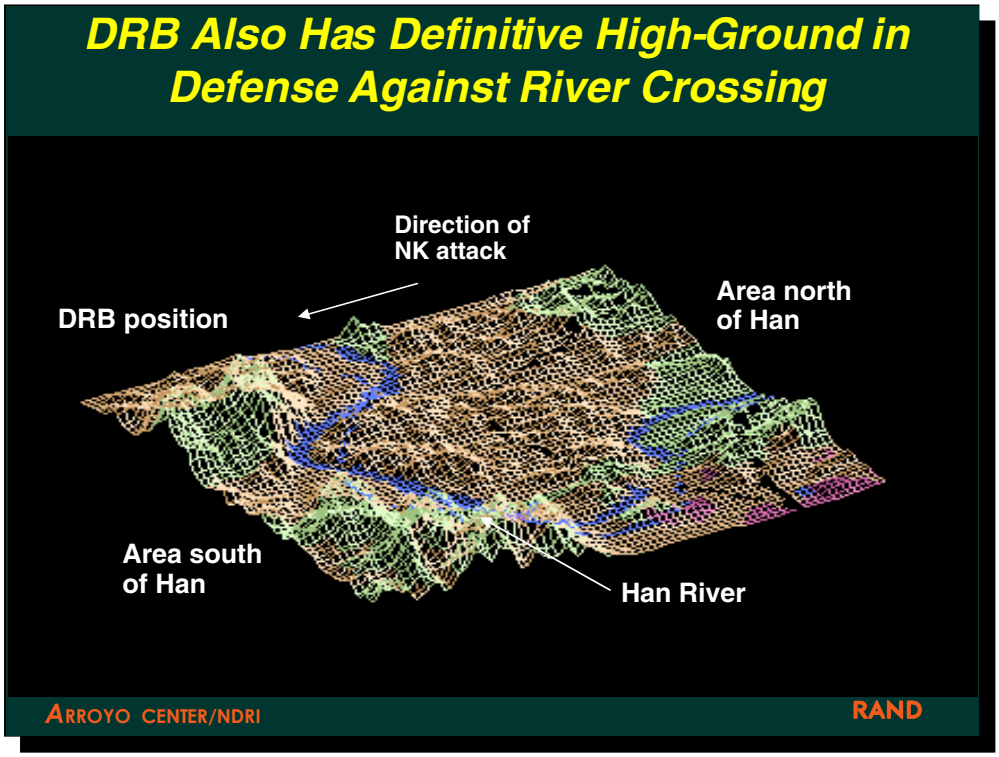

The above image gives some indication of the terrain elevation that surrounds the Han River. In addition to defending against a forced river crossing, it is evident that the DRB, which is positioned in the area south of the Han, also has the advantageous high-ground. This permits clear line-of-sight (LOS) down to the river during the NK combined forces attack.

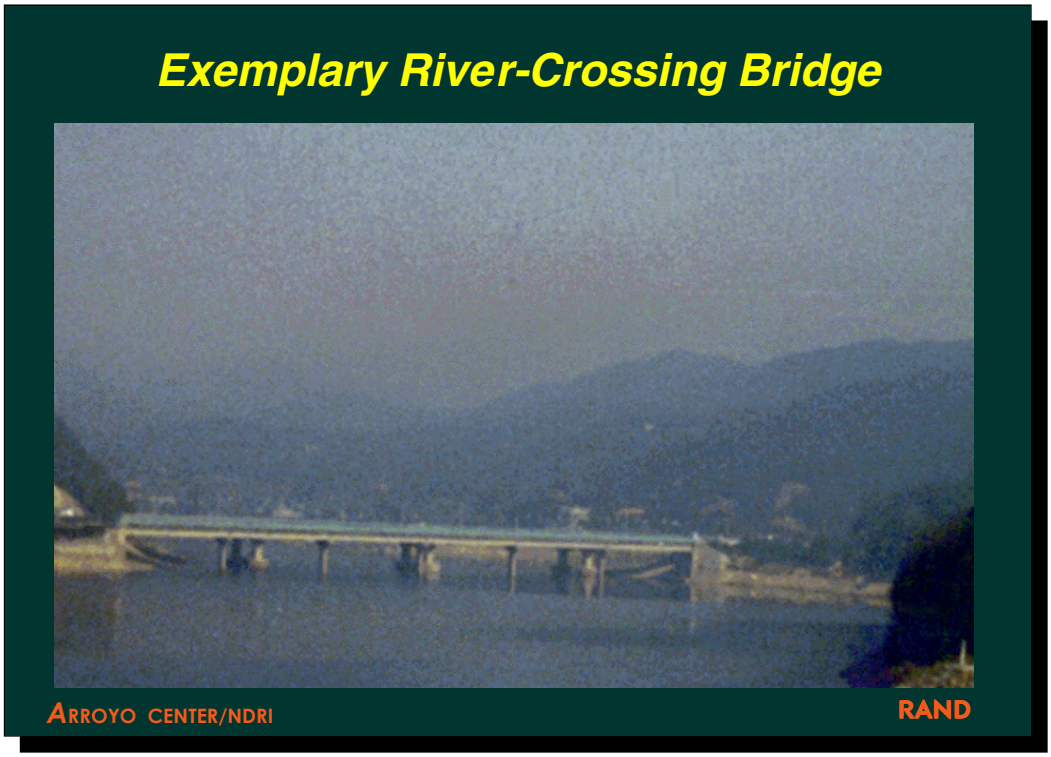

The above image provides some idea of the kind of bridge the NK forces must use to cross the river.[4] It can be seen from the picture that the bridge will support multiple vehicles crossing at the same time. Nonetheless, the combination of a "dug-in" position and the high-ground makes for a formidable defense. Additionally, it can be seen that the hills are covered with relatively dense foliage, offering even more protection.

[4]The bridge shown is not one of the two bridges explicitly referred to in our scenario, but it serves as a good example according to representatives from I Corps. Destruction of the bridge by Blue is not an option, because it is a valuable asset.

3. Methodology

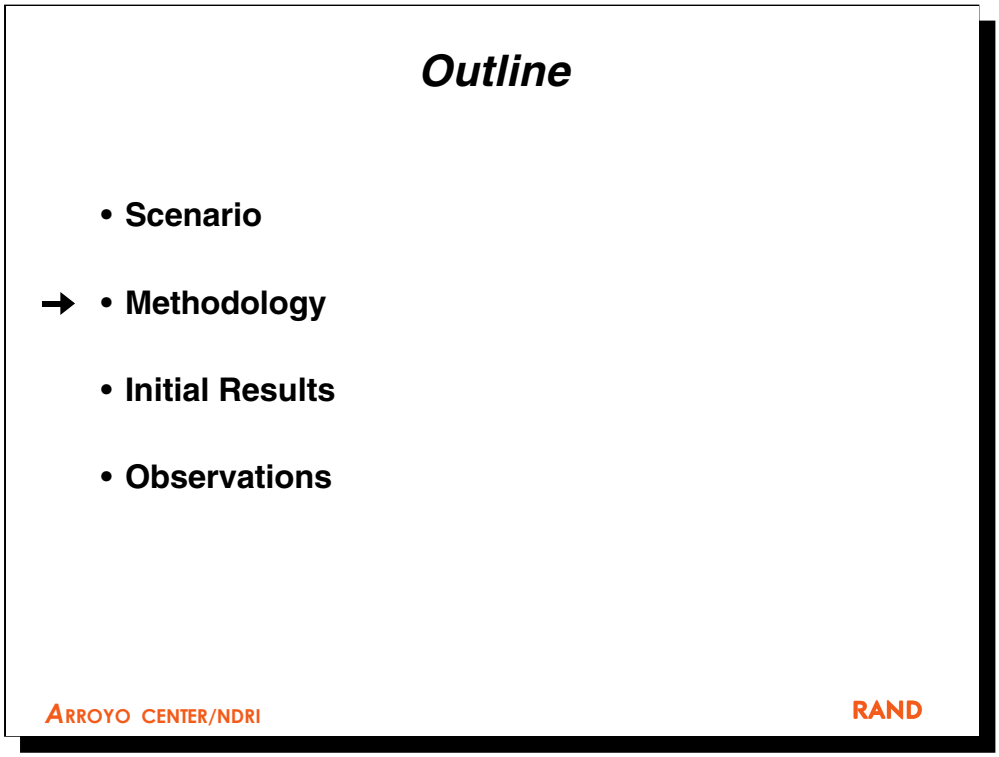

This section describes the basic methodology we used for the analysis of the ADAS.

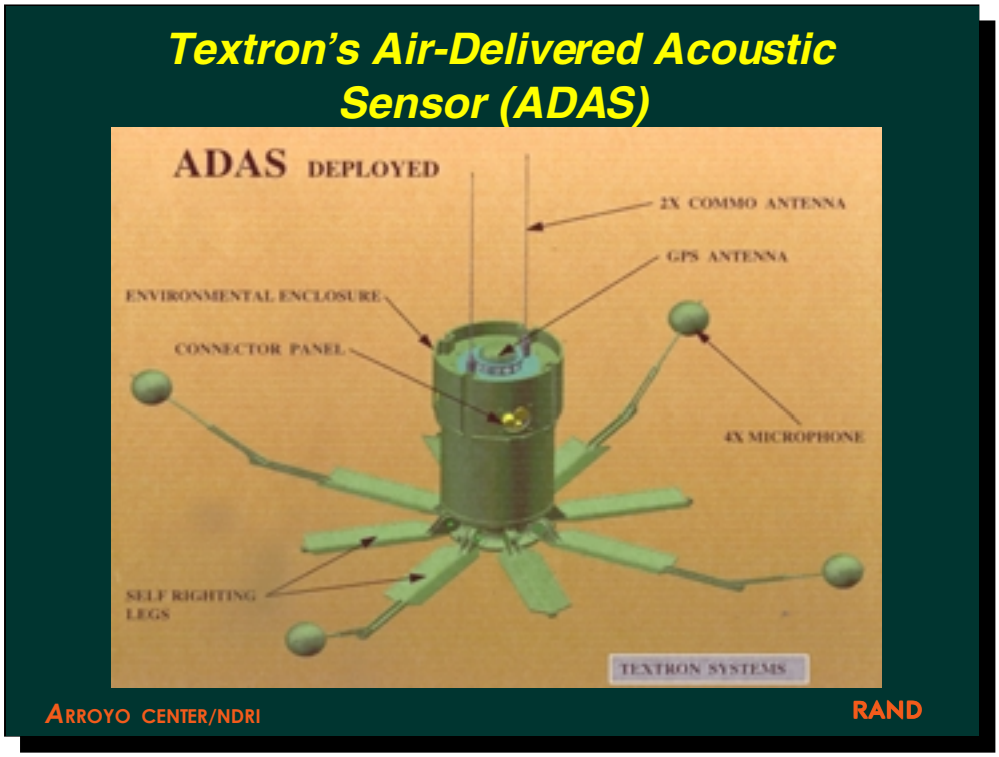

Although a number of acoustic sensors were initially proposed for use in the RFPI ACTD, the system ultimately selected by the RFPI decisionmakers was Textron's ADAS. The characteristics that largely governed its choice from among other alternatives was the ADAS's ability to both accurately locate armored vehicles *and* be deployed from aircraft. Prior to deployment the ADAS is similar in size to the wide area munition (WAM), which is also a Textron product (i.e., about 13 inches tall and 6 inches in diameter). When deployed from a helicopter or other aircraft the ADAS unit uses a parachute system to minimize its impact with the ground. Shortly after landing it automatically rights itself (in a manner similar to the WAM) and extends its microphones and antennae, significantly increasing its overall dimensions (to approximately 24 inches across).

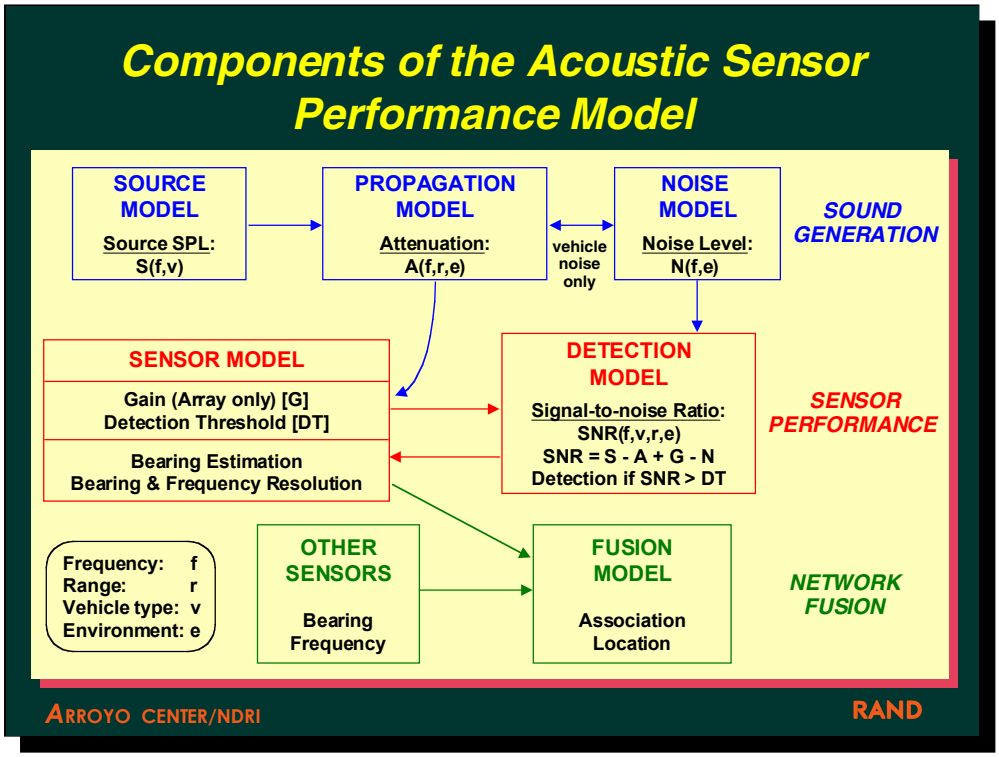

A new acoustic sensor model was developed to represent the performance of an ADAS network. A detailed description of this model is provided in the Appendix. The three-tiered framework depicted above shows the components of the model and the relationships between them.

Sound generation. This top tier consists of three components—source, propagation, and noise—that together determine what each ADAS sensor can hear. Unique acoustic signatures are assigned to target vehicles and then propagated to each sensor,[5] where the environmental noise level is calculated based on the ambient background noise[6] and local contributions from nearby vehicles.

---

[5]For a description of the underlying propagation model, see K. E. Gilbert and X. Di, "A Fast Green's Function Method for One-Way Sound Propagation in the Atmosphere," *Journal of the Acoustical Society of America,* Vol. 94, 1993, pp. 2343–2352. The validation of this model is discussed in D. C. Swanson, "Acoustic Detection Validation in a Desert Environment," the Fifth Battlefield Acoustics Symposium, *Conference Proceedings,* Fort Meade, MD, September 23–25, 1997

[6]The noise model and the data for the noise environments were provided by Textron Systems Corporation, and they are consistent with J. Heberley, *Acoustic Sensor Specification for RFPI,* U.S. Army Armament Research, Development, and Engineering Center, May 1995.

Sensor performance. The basic acoustic detection equation, adjusted to account for the gain provided by microphones and processing, is used in the middle tier to determine which sources are detected by each sensor. Based on details of the ADAS design, the bearing lines associated with each detection are estimated and their frequencies and bearing angles compared to determine which of them can be resolved.

Network fusion. Simulating the fusion process in this lower tier, where different sensor inputs are combined, was by far the most difficult task. Here, decisions must be made on the validity and accuracy of data from the sensor network, and how these data should be merged to provide targeting information. The fusion algorithm we developed for this purpose matches the acoustic frequency of detections made by different sensors in the ADAS network, and it uses the intersections of their bearing lines to estimate the locations of potential targets. (Suspected "ghost" targets—incorrect locations that are the result of mismatched bearing lines—and any points with poor intersection geometry are eliminated from this set.)

The existing theory on acoustic sensor performance, much of which was incorporated into our model, is substantial and well founded. By their very nature, however, these sensors' performance is highly dependent on both environmental conditions and sensor design. Thus, ultimately, empirical data will be needed to help shape this technology and guide how it is used on the battlefield. Such data were acquired during a series of field tests leading into the ACTD,[7] but a considerable amount of additional testing will be needed to capitalize on the full potential of acoustic sensor networks.

[7]These tests included two acoustic field experiments conducted at Fort A. P. Hill, VA, in 1996 and Yuma Proving Ground, AZ, in 1997 that were attended by one of the authors.

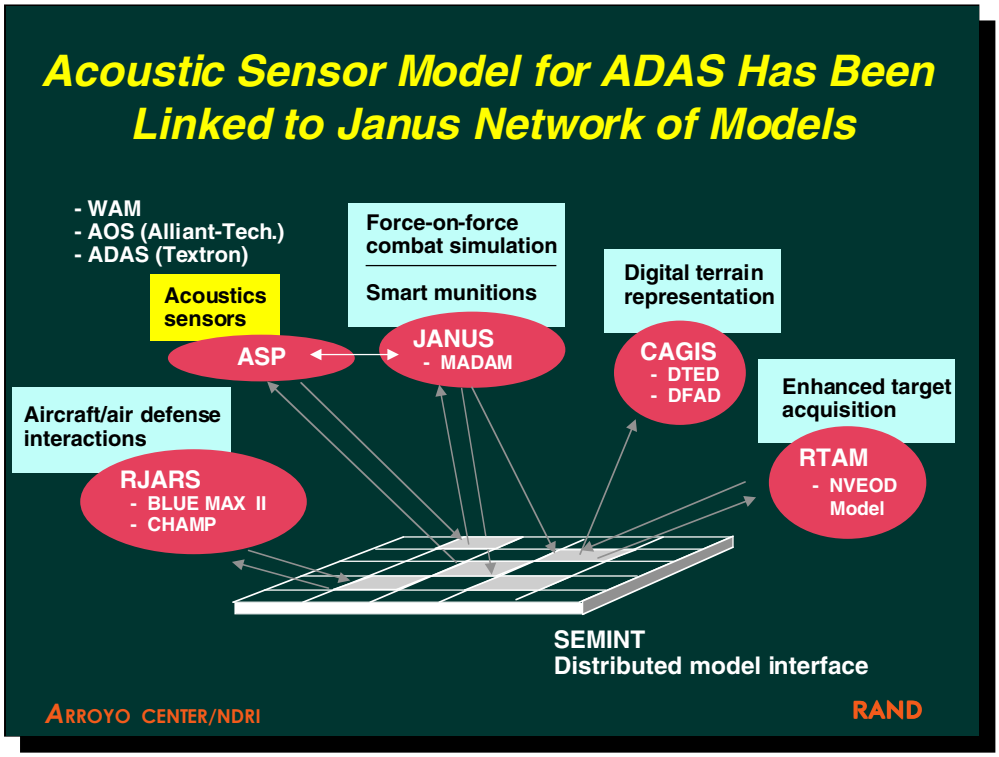

Prior to developing this extensive acoustic sensor model specifically for representing the ADAS, we had also modeled the acoustic capabilities of AOS, WAM, and the intelligent minefield (IMF). Looking at the bigger picture, these and other specialty models are all connected to Janus. This allows us to expand our analysis of individual sensors' performance in the few-on-few environment to a "system-of-systems" analysis in a many-on-many situation. Because we use a distributed model interface, referred to as the seamless model integration (SEMINT), we can maintain the high-resolution character of the sensor performance model, carrying this resolution into the larger force-on-force environment.[8] Since these models run on separate processors, there is computational flexibility as well.

[8]For a description of the distributed model interface, see J. Marti et al., *SEMINT: Seamless Model Integration*, Santa Monica, CA: RAND, MR-403-OSD/A, 1994.

4. Initial Results

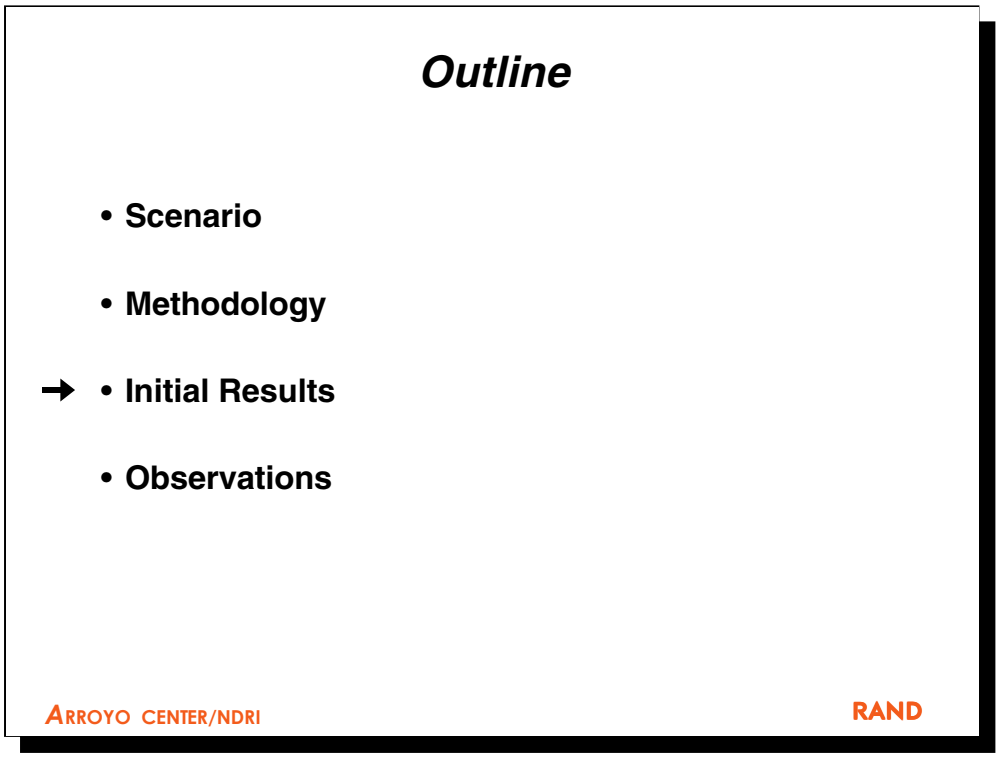

In the following section, we provide interim results from our initial analysis of ADAS.

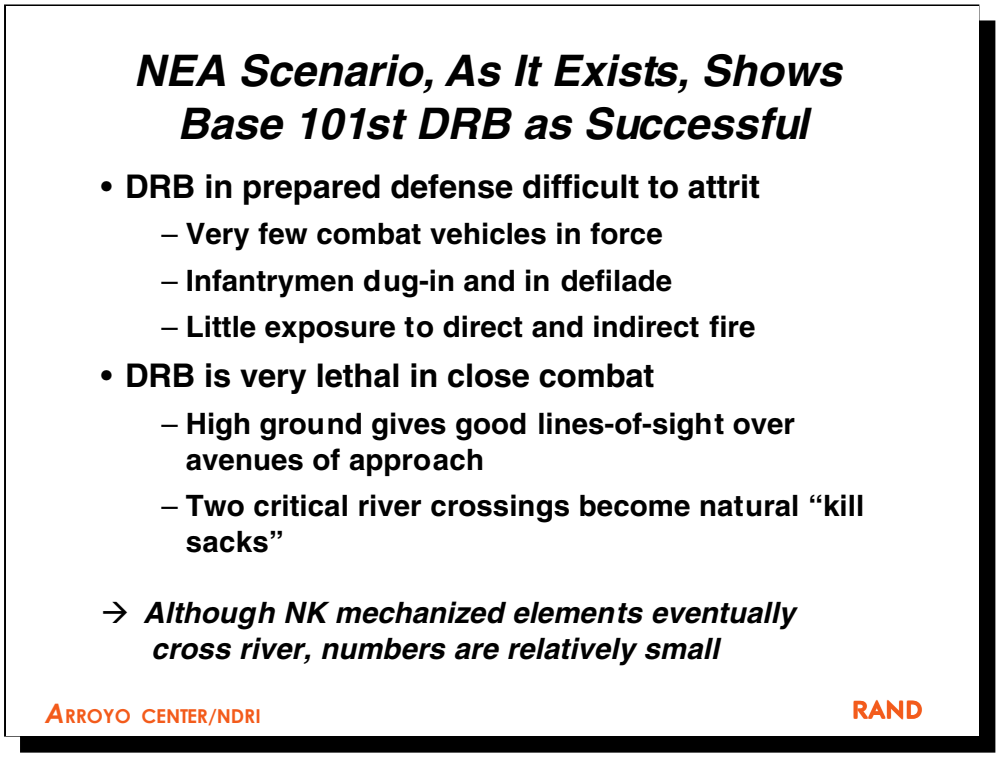

In designing our version of the NEA scenario, we realized early on that the U.S. force had a qualitative advantage (defense, dug-in, high-ground, foliage) over the NK force, which needed to perform a difficult forced river crossing. However, we also expected the DRB's advantage to be offset by the overwhelming size of the attacking NK force. As it turns out, our initial base case analysis shows that the 101st DRB is successful at holding off the NK force attack.

First, although the NK force employs considerable amounts of artillery, the DRB's prepared defense is sufficient to withstand the bombardment. Infantrymen were dug-in and in defilade, making them very difficult targets for both direct and indirect fire. Second, the DRB was seen to be extremely lethal in the close fight. Its high-ground gave clear LOS over the bridges. Because the NK force could only achieve its objective through a forced crossing over the bridges, this resulted in a natural "kill sack." Although several NK units did manage to push across the river, they were few in number. Thus, the base DRB was seen as being successful in its defense.

Scenario Was Made More Stressing for Analytic Purposes

- **DRB was dramatically reduced in size**
  - **U.S. ground force located on high ground, south of river, reduced to half size (e.g., FAE)**
  - **Air platforms and ground forces north of river left unmodified**
- **Number of river crossings were doubled (from two to four)**
  - **NK attack occurs with significantly greater "mass" effects and simultaneity**
  - **DRB dispersed, covering greater area with less interlocking fires**

ARROYO CENTER/NDRI RAND

Part of the overarching objective of our research has been to assess the performance of new technologies, such as ADAS, in stressing situations. Because the base DRB in this case was able to accomplish its mission, defend and repel the NK attack, the original scenario we designed, based on TRAC scenarios, did not meet the criterion of a stressing situation. So to make the scenario more stressing, we changed two of its critical parameters. First, we reduced the size of the DRB ground force to roughly half its original size.[9] Second, we doubled the number of river crossings available, from two to four. Together, these changes dramatically shift the advantage to the NK force.

[9]One might argue that this could be achievable if the NK forces were aware of the DRB location and employed a large-scale strike weapon such as fuel air explosives (FAE).

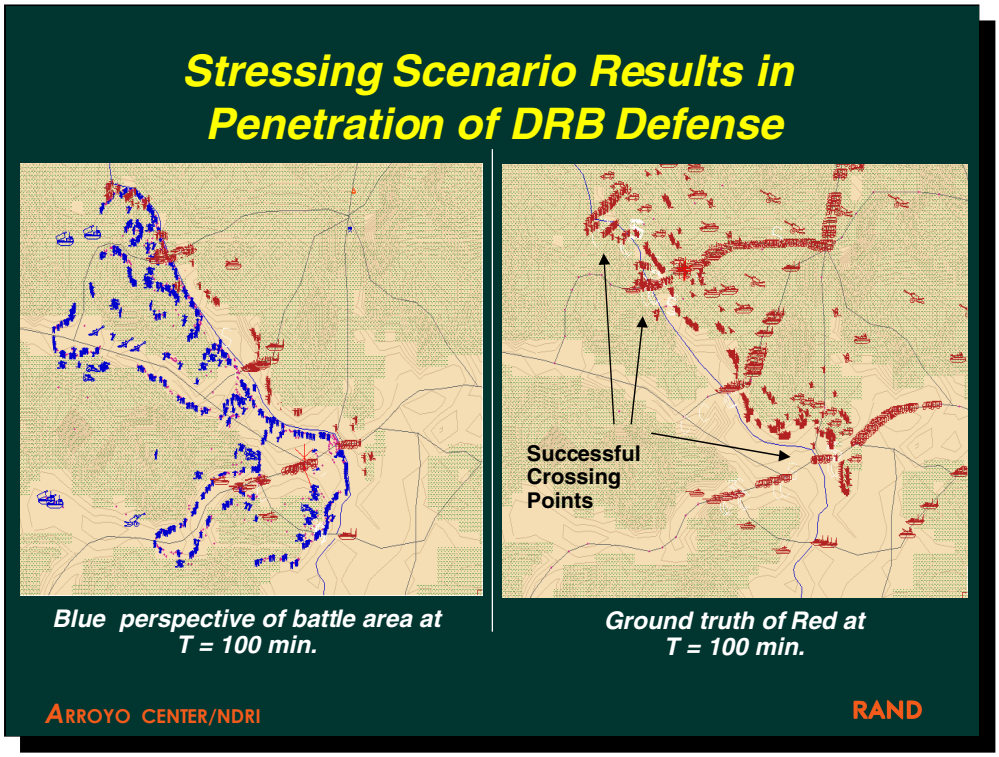

Once modified, the scenario does become considerably more difficult for the DRB. Although the reduced-size DRB still achieves a very high loss-exchange ratio (LER), it does not succeed in its mission to defend and repel the attacking force. The Janus screen images shown above, at 100 minutes into the simulated battle, provide a good indication of the outcome of battle. Although much of the DRB is still intact, it is evident from the image on the left that the attacking force has successfully breached the DRB defense in three of the four crossing points (the image only shows Blue units and those Red systems visible to Blue).

Even though a fairly large number of NK forces were attrited during the attack, the Red-viewpoint image on the right shows that many more forces are well positioned to exploit the initial breaches. Most notably, in this case the terrain and foliage force the DRB to use its direct fire weapons relatively close in. Analysis from the simulation reveals that most of the attrition is from the Javelin gunners. Longer-range systems in the DRB are generally not fully used because of the limited ability of the DRB to target at range. ADAS represents one possible addition to the force to correct for this "gap" in capability. In some ways, ADAS is much better suited for this scenario than stand-alone imaging sensors because it can be air emplaced and, because it is not necessarily LOS-restricted, can be less sensitive to terrain and foliage blockage.

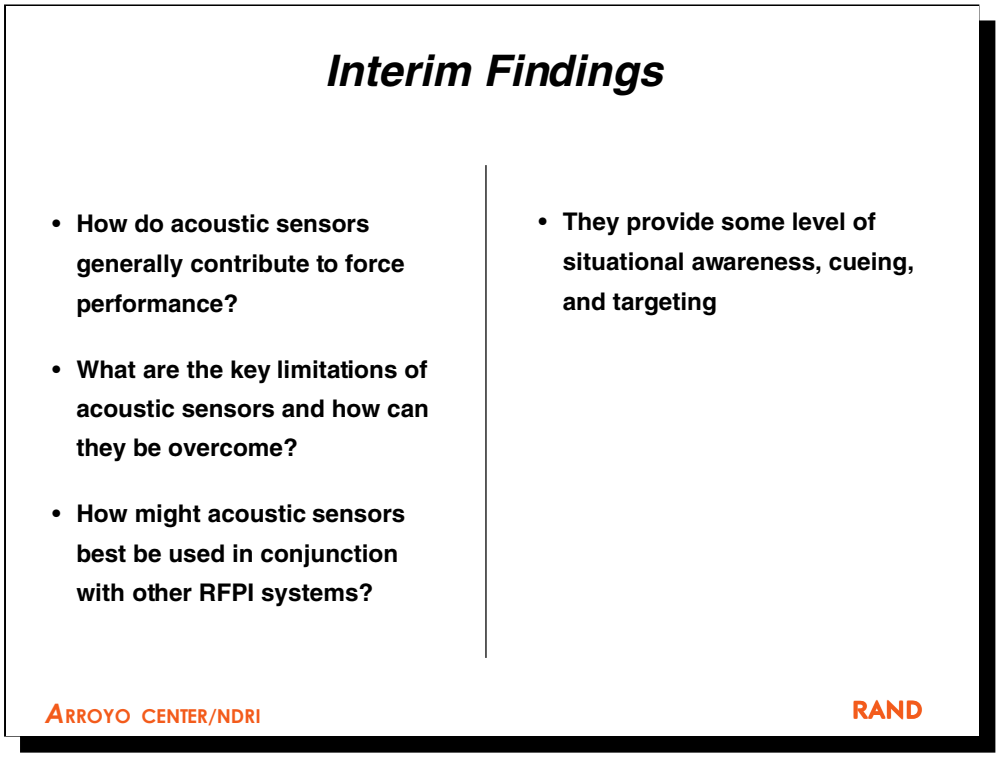

Turning to our first research question, "How do acoustic sensors generally contribute to force performance?" we found that they have the potential to provide information at many levels, including broad situational awareness, cueing for other RSTA, and even detailed targeting information for weapon systems. In conjunction with this answer, we also found that, like most other battlefield sensors, the performance of an ADAS network is largely dictated by the environmental conditions in which it operates.

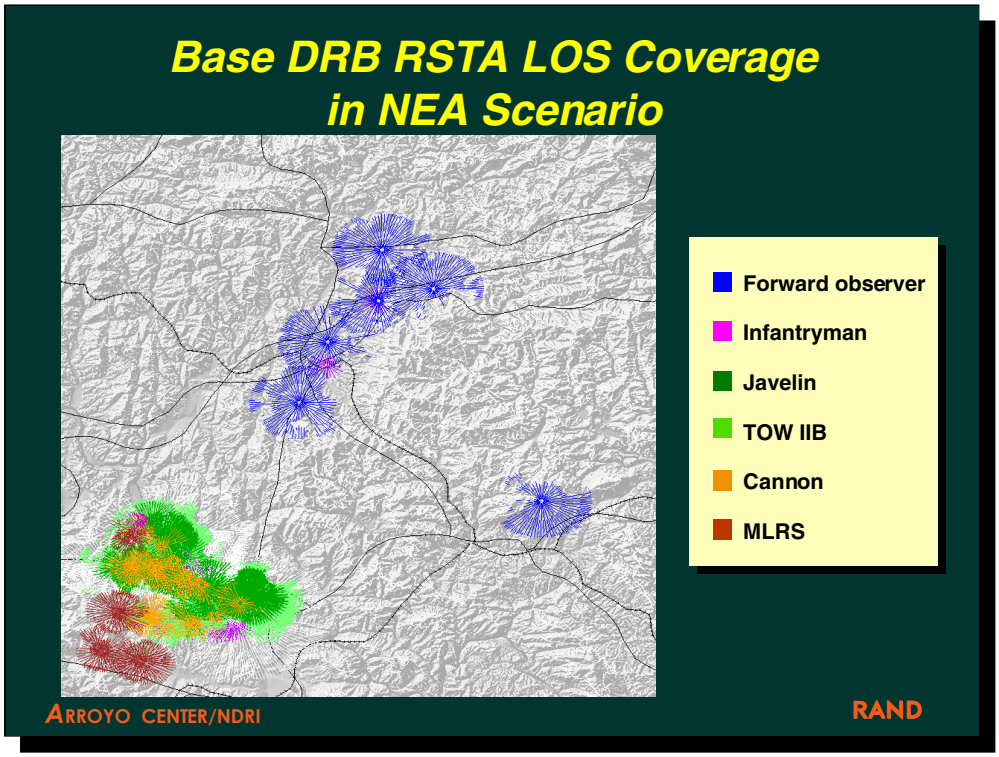

The image above shows an overview of the LOS region covered by the base DRB's RSTA assets (in very favorable environmental conditions). The FOs, equipped with advanced forward looking infrared sensors (FLIRs), provide most of the deep coverage. The infantry units that accompany the FOs also provide some coverage. The majority of the remaining organic systems associated with the DRB provide the close-in coverage.

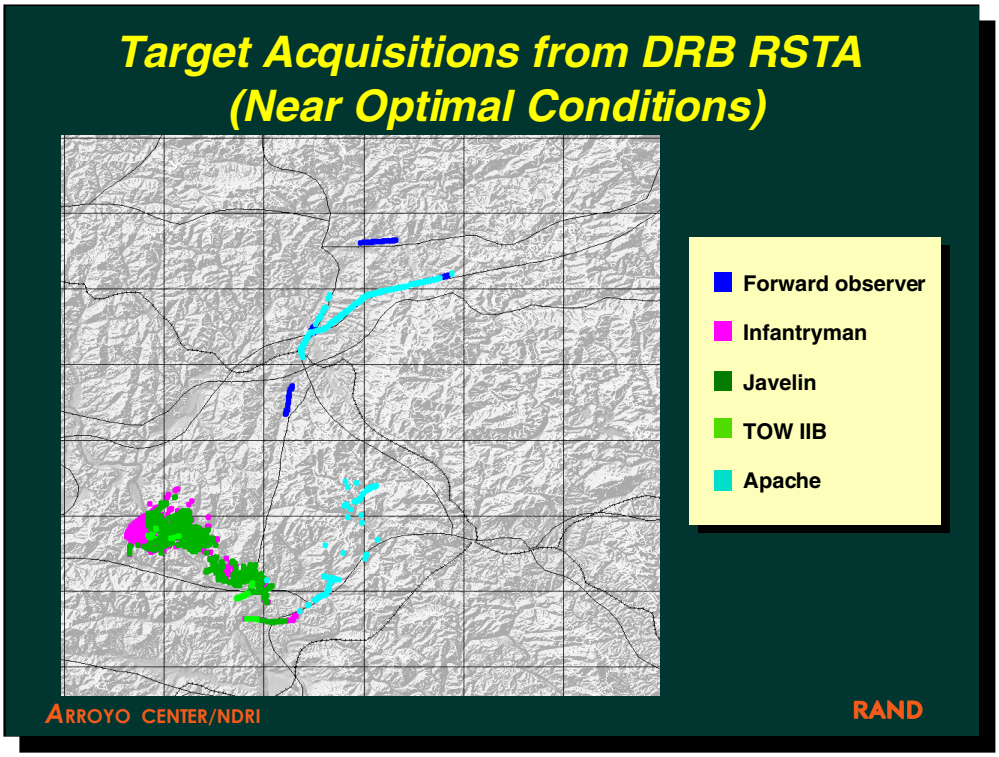

The image above shows the actual locations of target acquisitions by sensor type, cumulative over a single run of our simulation. It is quite clear that the DRB's RSTA network provided a fair number of deep and close acquisitions of the NK force attack. It is also apparent that there are significant gaps in the intermediate area, between the deep and the close. The gap exists largely because of the presence of the NK infantry force spread out in this area. This area is reasonably well protected and, therefore, would preclude a significant manned presence. It was envisioned that ADAS could provide some coverage to fill these gaps.

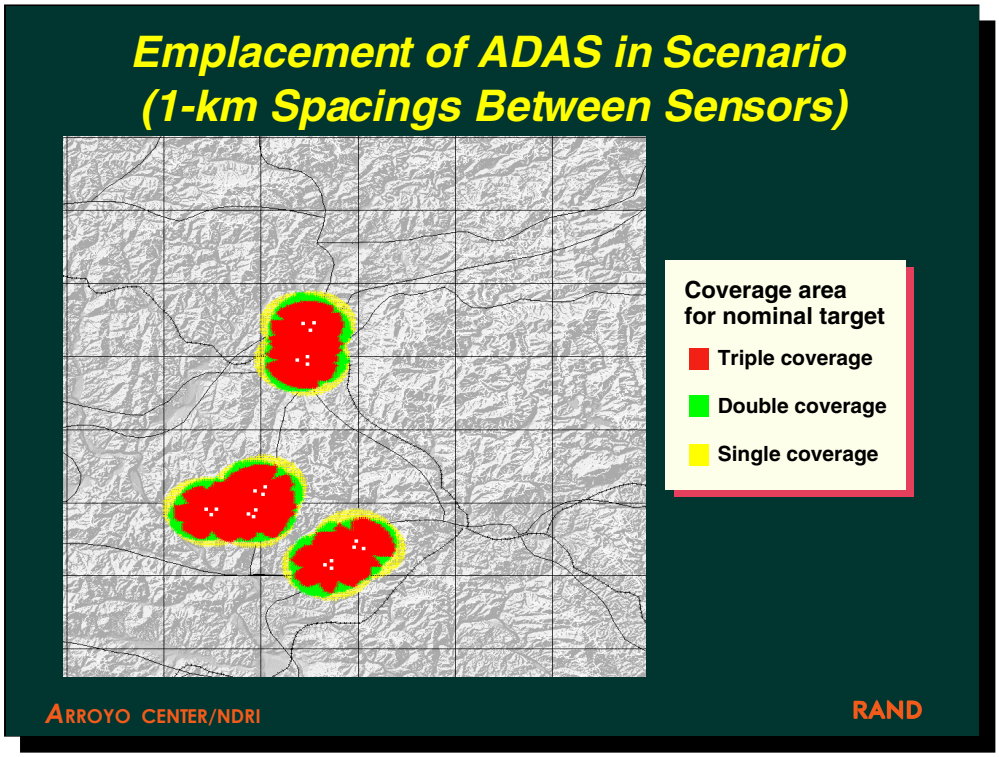

Consultation with representatives of DBBL yielded the above placement of the specified seven sets of three ADAS (a total of 21). The location of the sensors is shown, along with the respective coverage areas for a nominal target. The deeper-positioned ADAS were placed along the roads at two "critical" intersections. The closer-in ADAS were spread out to enhance the DRB's coverage of the approaches to the river crossings.

In accordance with existing developer guidance, these sensors were employed in groups of three. Within each group, the three sensors were spread out to form an equilateral triangle with a separation of one kilometer. Information from the sensors is communicated to a gateway node and then passed on to the force's tactical operations centers.

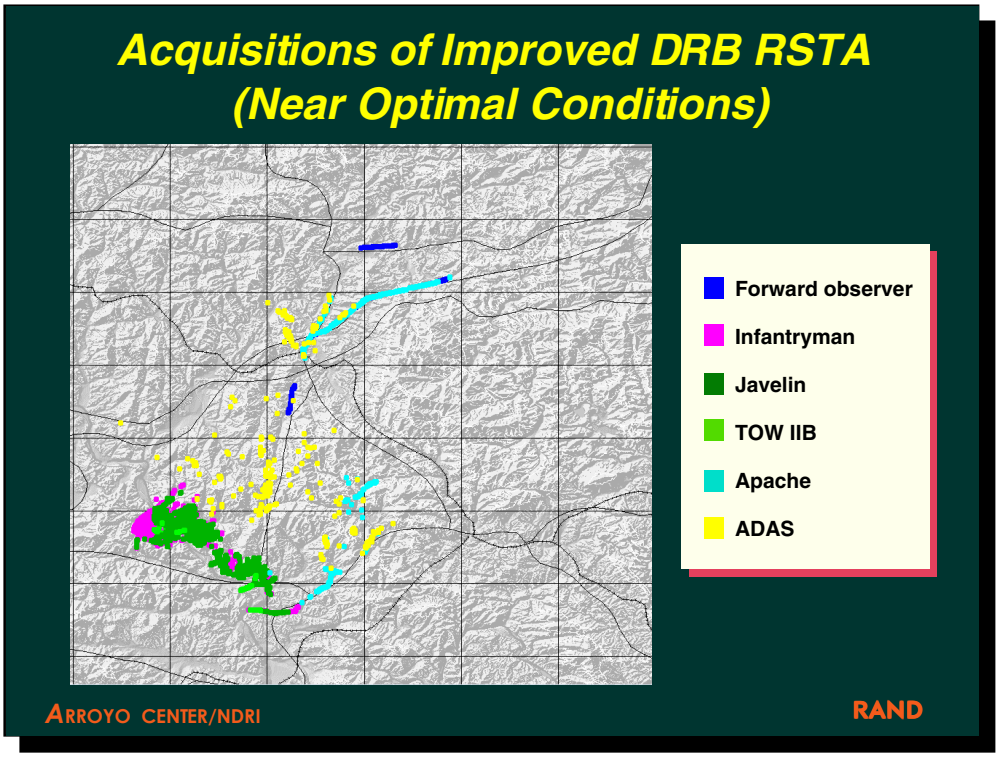

The cumulative target acquisitions by DRB RSTA with ADAS added to the force are shown above. As can be seen from this image, the addition of the ADAS network resulted in much greater overall coverage of the battlefield, particularly in the intermediate areas. Although these acoustic sensors do a good job of covering this area, they do so with much less precision than imaging sensors. There are also several ghost targets—the result of incorrectly matched bearing lines—located well off the roads where no vehicles were present.

The key advantages of ADAS over other DRB sensors are (1) its ability to cover areas beyond LOS, providing situational awareness, cueing, and targeting, (2) its ability to be rapidly emplaced (in this scenario either by FOs en route to their deep positions or via helicopter delivery),[10] (3) their relatively stealthy presence once deployed (except for low-power, burst radio emissions), and (4) their relatively low levels of required maintenance. These aspects are especially important in this scenario because the areas in which they are emplaced are expected to be patrolled by dismounted infantry.

[10]Hand emplacement or deployment by helicopter can each be risky if performed close to the threat forces.

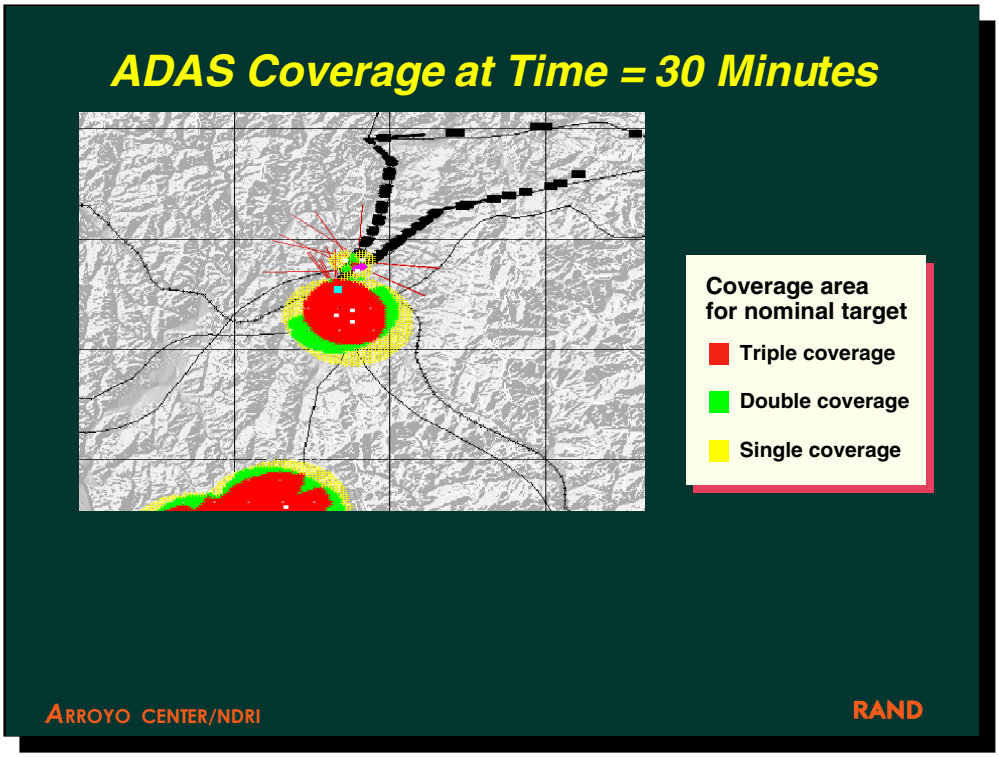

An interesting phenomenon occurred during the actual running of the simulation. At 30 minutes into the scenario, the NK mechanized forces, shown generically by the black icons above, have entered the area covered by the first ADAS grouping. Because the targets have clear signatures, they generate several bearing lines and corresponding acquisitions. However, at the same time, the targets close to the ADAS also produce broad-band signatures, which effectively raised the local noise floor. As a result, the ADAS's ability to acquire targets at longer ranges was greatly diminished. Thus, the total coverage area of the first sensor grouping was substantially reduced, as shown by the image above.

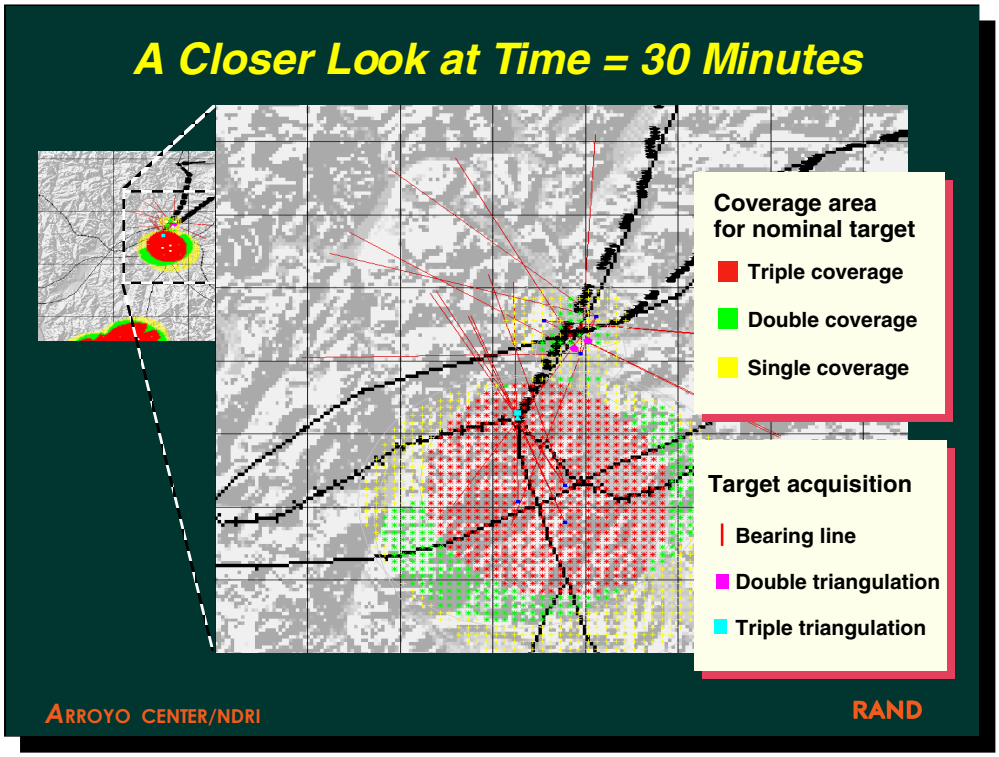

A closer look at the simulation image provides more insights into what is happening. Indeed, when the targets are either near or directly within the ADAS grouping, the acquisition range for sensors in the grouping is reduced substantially.[11] At the same time, however, the ADAS are still able to successfully acquire the targets that are close to them. As shown by the image above, many bearing lines are generated and several triangulations are successfully made, some involving only two sensors, others involving all three within the grouping.

[11]It should be noted that generation of the bearing lines and triangulations derive from field data and calculations, such as the Cramer-Rao lower bound relationship (recommended by Textron) described in V. H. McDonald and P. M Schultheiss, "Optimum Passive Bearing Estimation in a Spatially Incoherent Noise Environment," *Journal of the Acoustical Society of America*, Vol. 46, 1969, pp. 37–43. The computation of changing coverage areas due to vehicle noise is performed in the simulation.

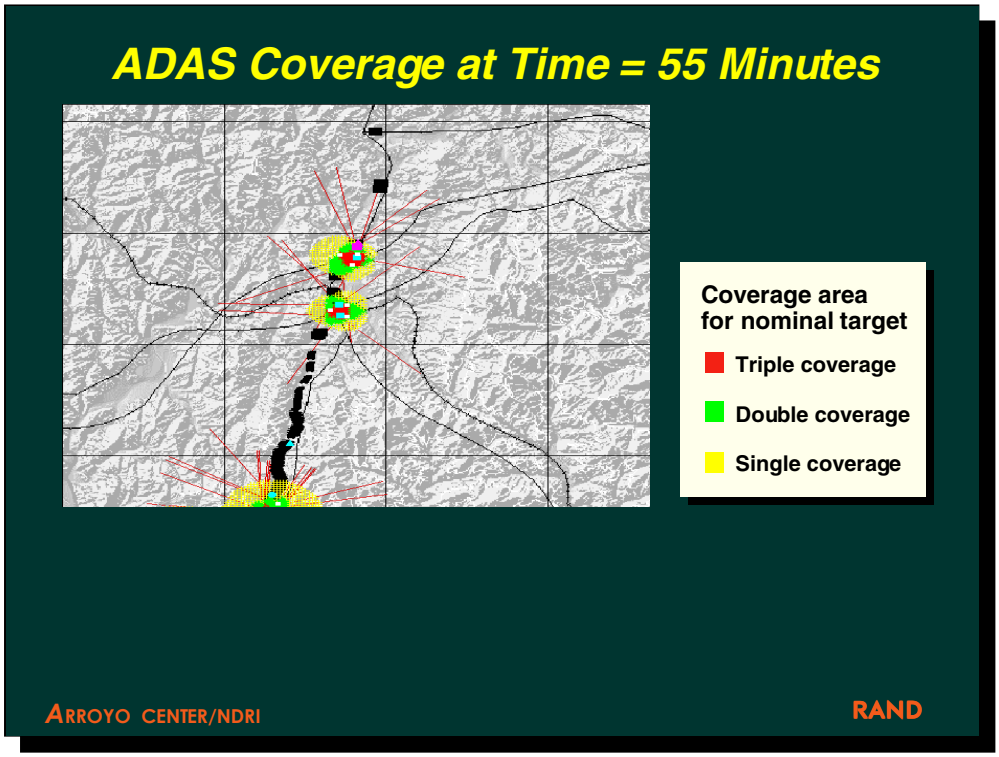

At a later time (55 minutes into the simulation) as the NK road march continues, many of the ADAS groupings are simultaneously affected. On the whole, the coverage provided by the ADAS network is now only a small percentage of the original coverage shown before. Even though the coverage is greatly reduced, it is worthwhile to point out that the lead targets are usually successfully acquired, and as the targets in the column pass through the ADAS groupings, the predominant ones are also typically acquired. These are typically the loudest targets, such as tanks, BMPs, and tracked air defense vehicles.

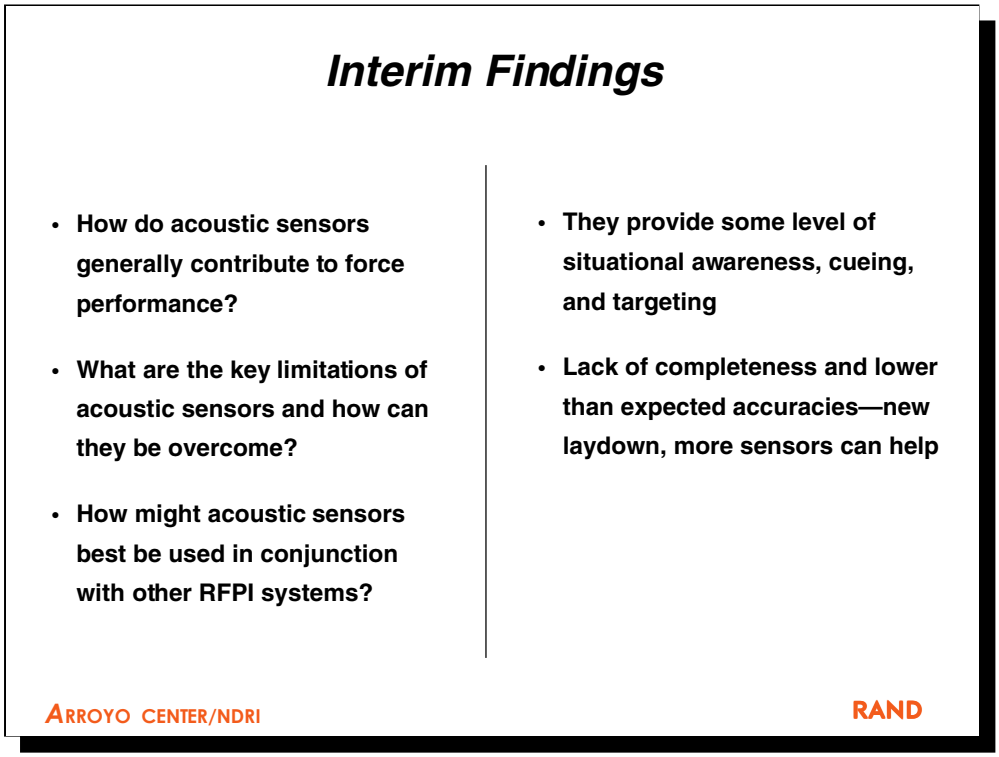

The second research question really combines two questions, "What are the key limitations of acoustic sensors?" and "How can these limitations be overcome?" From our assessment, two key limitations of acoustic sensors are (1) significant errors in acquiring targets—too many targets are missed, which we call lack of completeness of information, and (2) significant target location errors. Both of these limitations were a strong function of the "baseline" pattern of emplacement. We found that by modifying the laydown, mostly by adding more sensors, both of these limitations could be reduced.

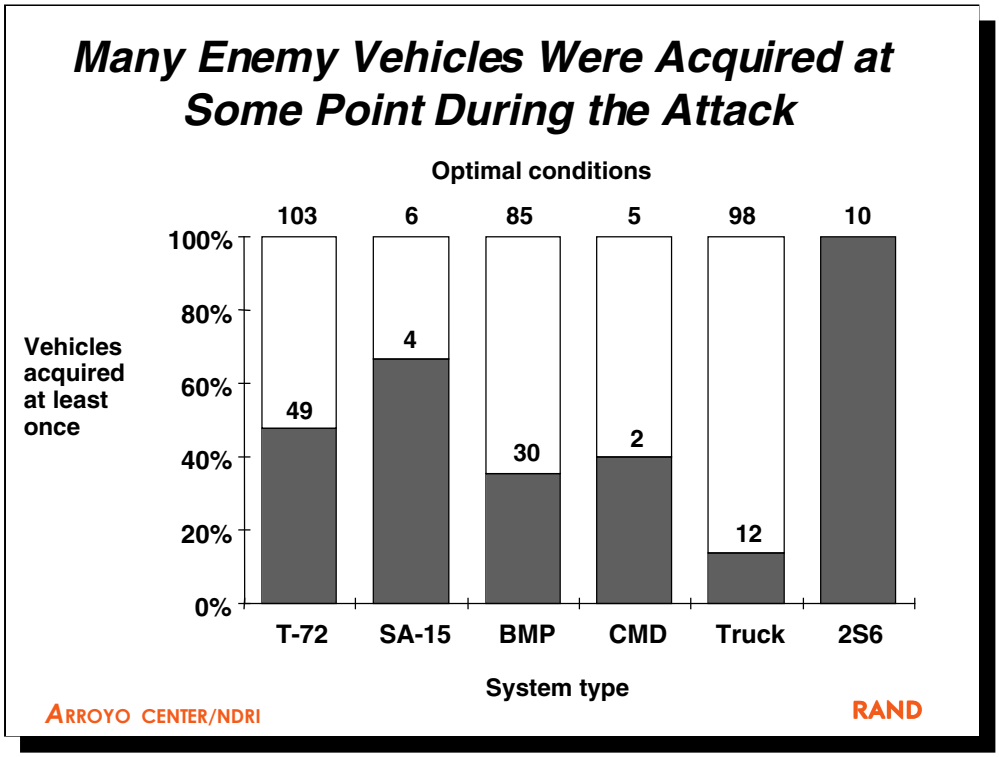

With regard to the first limitation, lack of completeness, we saw from our simulation that at some point during the NK mechanized road march to the Han River, a fair percentage of vehicles were acquired at least once, especially vehicles with characteristically loud or unique signatures, such as T-72s, SA-15s, and 2S6s. On the other hand, vehicles with comparatively lower sound signatures were often occluded by the louder ones. In the case of trucks, for example, only 12 percent were acquired during the 100-minute march to the river.

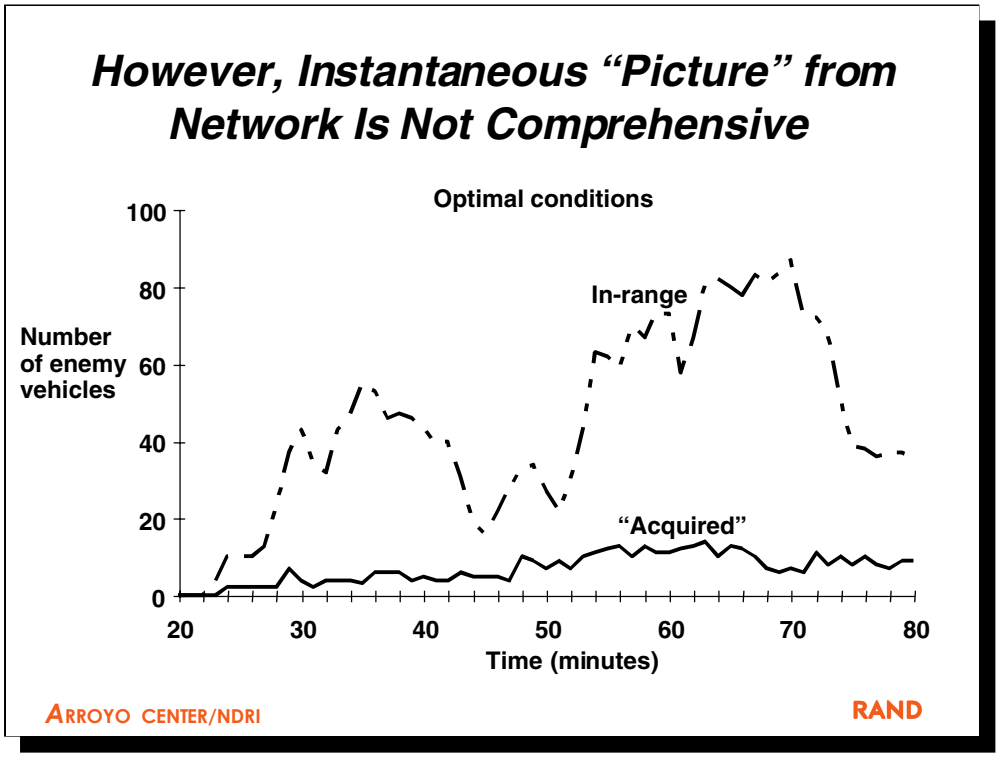

Another way to assess the "completeness" of information provided by an ADAS network is to examine the percent of possible acquisitions achieved at each point in time. With the sensor laydown shown before, the results from our analysis show that the total number of targets acquired by the ADAS network is substantially smaller than the total number of targets actually within its range. For example, at 30 minutes into the attack, 43 targets were within the range of the ADAS network, but only 4 of these targets were acquired.

This phenomenon is explained by the limited number of bearing lines that each ADAS sensor can produce (where both acoustic wave properties and sensor design collectively define the number of bearing lines available). Even if every bearing line were correlated correctly, which is a highly optimistic assumption, there still would not be enough lines to fully characterize the target set in this scenario.

From a battlefield perspective, especially for target-rich environments, these sensors can become "saturated" fairly easily, resulting in an underestimation of enemy presence. Thus, if used alone as a hunter in the hunter–standoff killer concept, without the benefit of other types of sensors, an ADAS network could provide misleading information that might lead to an inappropriate weapon response.

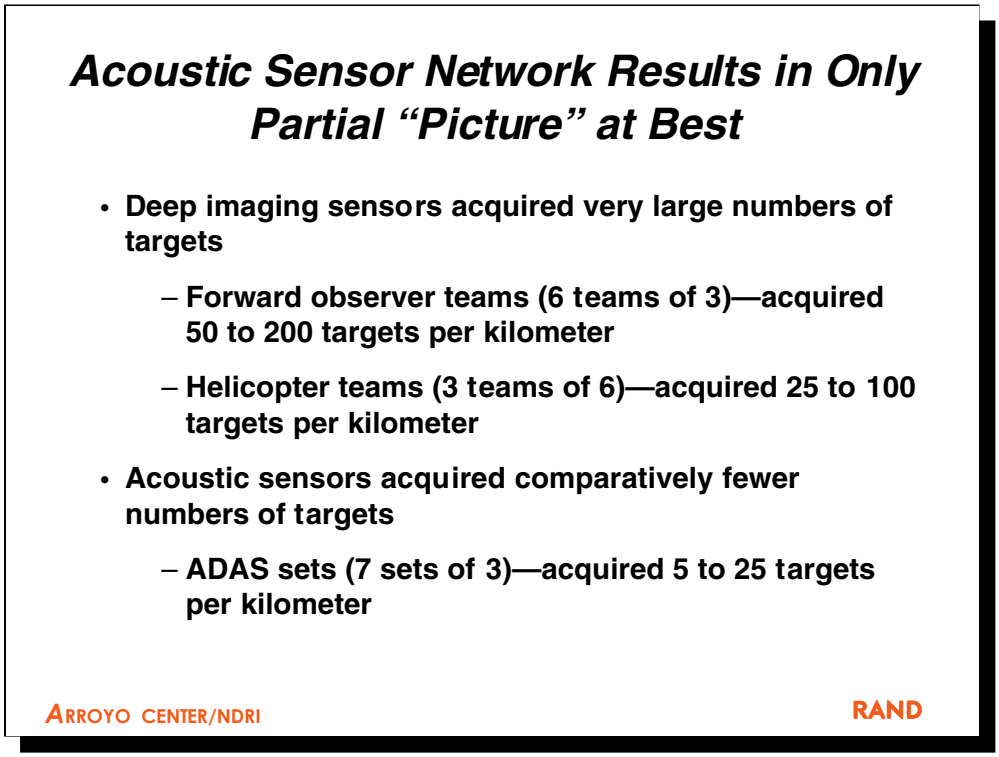

In comparing acoustic sensors to imaging sensors, the differences in level of completeness are quite striking. The 18 (6 teams of 3) well-positioned FO units equipped with high-quality (e.g., second-generation) FLIRs were able to acquire anywhere from 50 to 200 targets per kilometer, over the area that they covered. The 18 (3 teams of 6) Apaches, which were LOS limited because of their nap-of-the-earth flying, were still able to acquire from 25 to 100 targets per kilometer covered. In contrast, the 21 (7 sets of 3) ADAS only acquired 5 to 25 targets per kilometer, including *ghost* targets. Thus, a substantial change in the way we think about conducting fire missions may have to be considered when ADAS is used as a *hunter*.

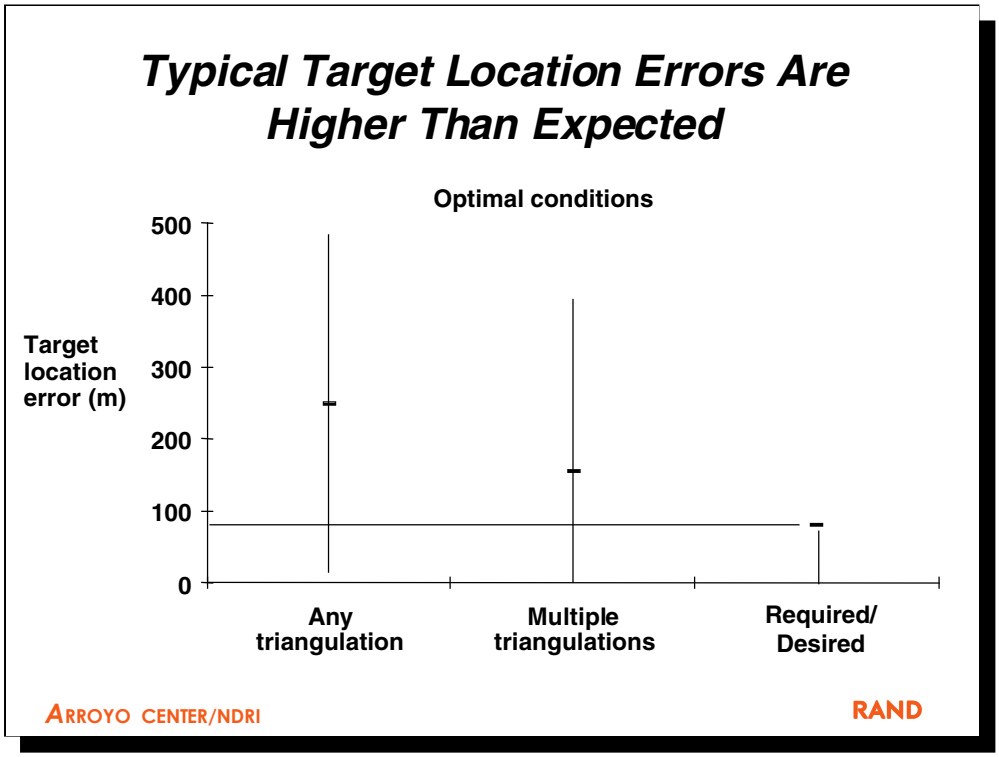

In addition to the potential lack of completeness, the ADAS system also had much higher target location errors (TLEs) than expected. If any triangulation occurred between bearing lines (either two or three sensors), the resulting TLE averaged around 250 meters.[12] When only multiple triangulations (i.e., those involving three or more sensors) were considered, the TLE was reduced to an average of 160 meters—still twice the required/desired level. It is also worthwhile to note that the range of TLE values remains large, extending from near zero to hundreds of meters (due mostly to ghost targets), even when only multiple triangulations are included.

[12]TLE here is defined as distance between triangulation point and closest actual target.

Performance of Network Degrades with Less Favorable Environments

- **Changing from optimal (night) to nominal (afternoon) conditions**
  - **Area of expected coverage goes down about 40%**
  - **Degree of "completeness" decreases by about 20%**
  - **Target location errors increase by about 15%**
- **Adding modest levels of wind had varied effects on performance**
  - **Area of coverage and degree of completeness can either increase (upwind) or decrease (downwind)**
  - **Target location errors typically increased**

ARROYO CENTER/NDRI RAND

Up to this point, we showed the results of ADAS performance in what might be considered favorable conditions (night). When we assessed ADAS in less favorable conditions (midafternoon), we saw some degradation in performance; however, this degradation was not as severe as we expected. For example, the total area covered by the network was reduced by about 40 percent. The degree of completeness only dropped by around 20 percent, and the TLE increased by only 15 percent. Not surprisingly, the introduction of wind had varied effects on ADAS performance. In some cases, wind could actually improve performance; in others, there was some decrease in performance. Typically, the TLEs on average increased.

Admittedly, we did not consider the worst environment for these sensors (e.g., rain, snow, etc.). Also, we did not have data to fully characterize the impact of dense foliage on acoustic wave propagation. Thus, our less favorable case should be interpreted as just another representative case and *not a lower bound*.

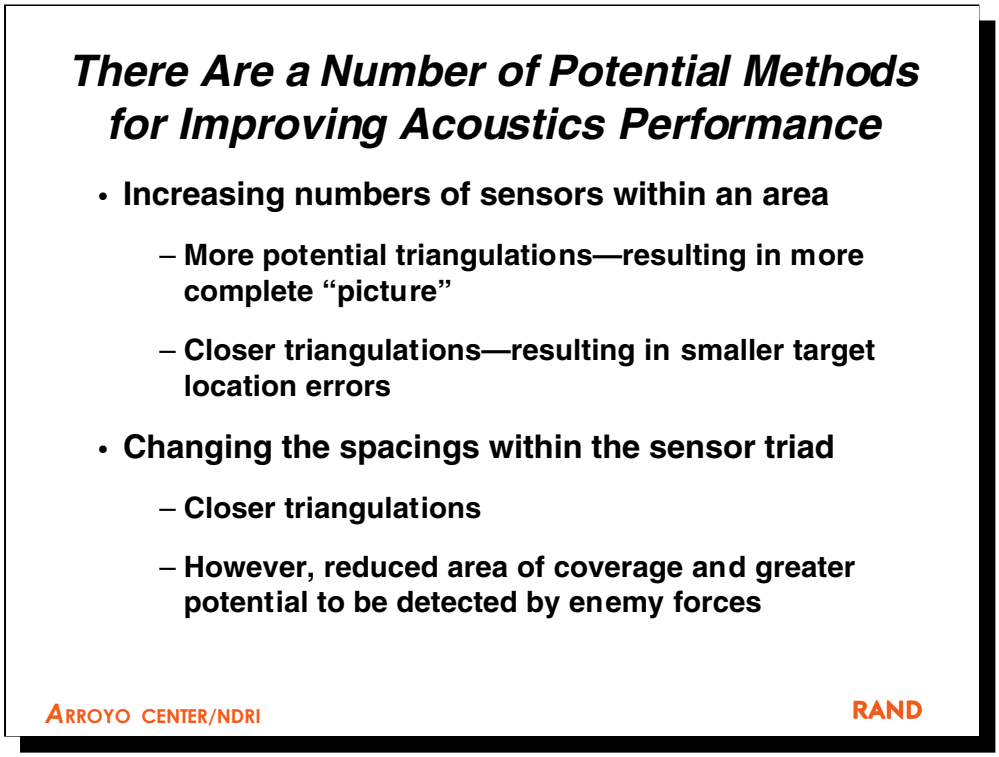

Although the initial laydown of acoustic sensors provided some idea of the strengths and weakness of ADAS, this can potentially be corrected. Along these lines, we explore two different ways to improve the ADAS network: (1) increase the number, and therefore density, of ADAS and (2) alter the spacing between the ADAS.[13]

For the first case, an increased density of ADAS can, in theory, solve both limitations seen before. More sensors per unit area should help to increase the number of possible bearing lines, which in turn would increase the number of potential triangulations and increase the total number of possible acquisitions. Also, a side benefit of an increased density in the acoustic sensor network would allow triangulations to occur closer to a sensor, which in theory should reduce the TLE.

The second alternative, reducing the spacing between the individual ADAS units has, in theory, a number of pluses and minuses. On the plus side, because the sensors are closer together, triangulations would likely be closer in, resulting in smaller TLEs. On the minus side, bringing sensors closer together reduces the overall area of coverage. Another tactical disadvantage in our scenario is that sensors, if uniformly distributed, would be closer to the roads and, therefore, somewhat easier to for passing vehicles to detect.

[13]At the request of the sponsor, we are also examining the possibility of fusion with the road network (here the model assumes that the target lies on the intersection of the bearing line and the nearest road).

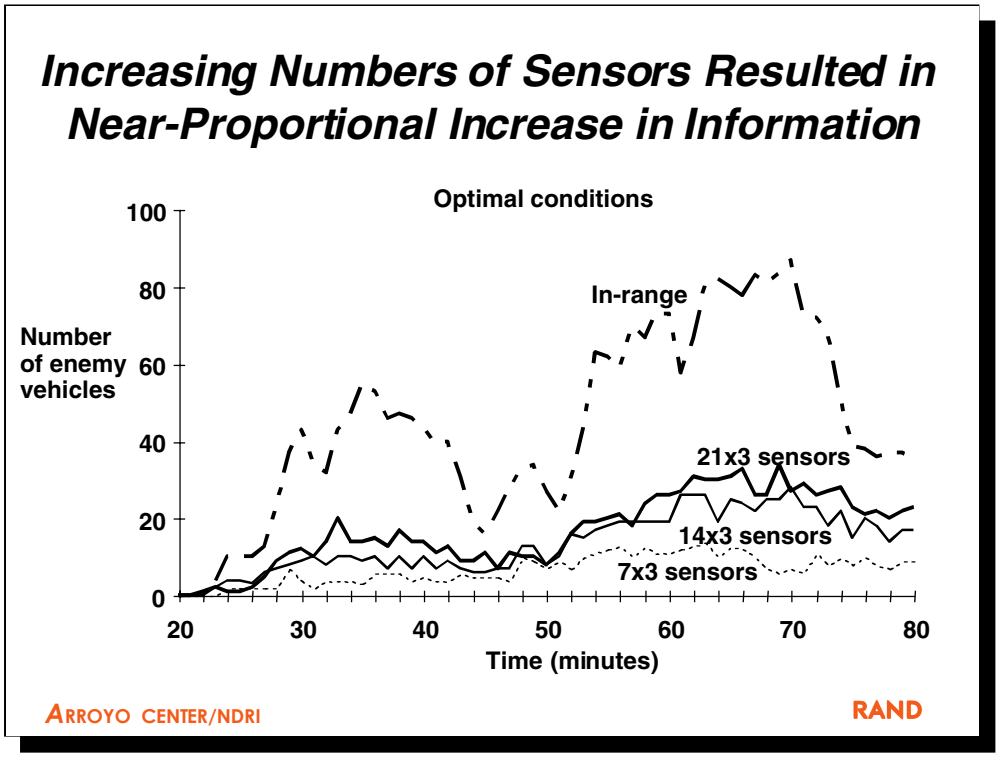

Increasing the number of sensors in this scenario provided a near-proportional improvement in the performance of the network. As shown by the chart above, doubling the number of sensors from 21 (or 7 sets of 3) to 42 (or 14 sets of 3) nearly doubled the number of total acquisitions. Tripling the number of sensors to 63 (21 sets of 3) further improved the performance.

Comparing performance, at 30 minutes into the simulated battle, only 4 targets were acquired by the 21-sensor network, as noted earlier. At the same time in the battle, the 42-sensor network provided 9 acquisitions, and the 63-sensor network provided 12 acquisitions. In all cases at 30 minutes, the ADAS network is still acquiring a significantly lower number of targets than the "ground truth," which includes 43 targets. However, increasing the number of sensors represents one possible solution for dramatically improving the completeness of information. Of course, this may engender problems with increased communications bandwidth requirements and processing demands.

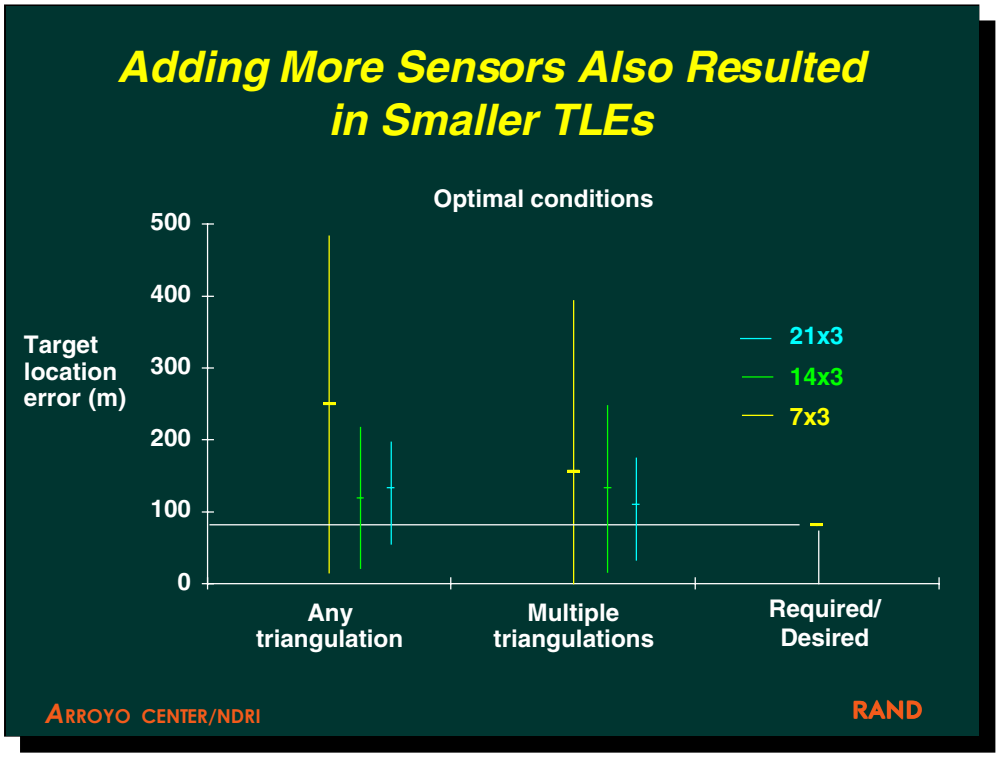

Another expected benefit from increasing the number and density of sensors within the battlespace is an improvement in accuracy as more acquisitions are made closer to the sensors, and the most misleading ghost targets are eliminated. These key improvements should reduce both the average and the range of TLE values. Although the denser 42- and 63-sensor configurations did not achieve the required / desired target of 80 meters, the average TLE for all triangulations was substantially lower in both cases. The range of TLE values was also much smaller for both laydowns because there were fewer ghost targets with large TLE values. [14]

[14]Note that for the more volatile combination of doubles and triples—the any-triangulation case—the target location error varies widely.

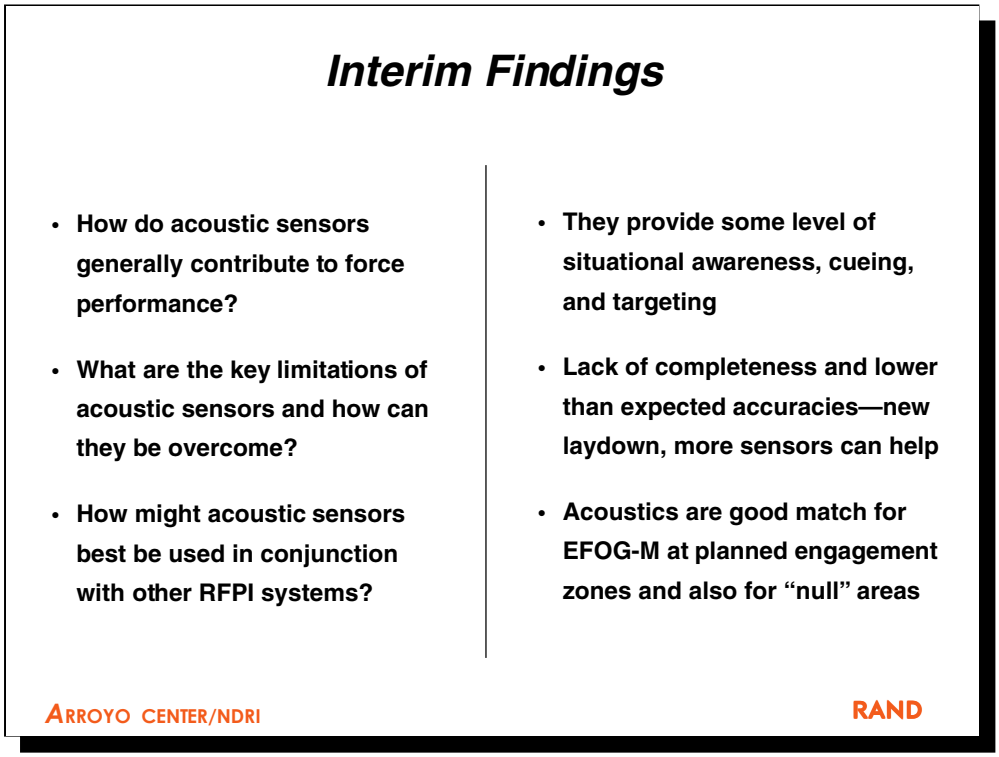

We are still actively researching the answer to the third question, "How might acoustic sensors best be used in conjunction with other RFPI systems?" This question is an open-ended one because the RFPI systems, their capabilities and possible applications, are not fixed. Nonetheless, initial analysis suggests that acoustic sensors are a very good match with large-footprint weapons such as EFOG-M. Although the required/desired levels of accuracy were not met, the EFOG-M footprint was more than adequate for successfully engaging targets. Another possible application for ADAS might be for covering "null" spaces on the battlefield. Because of its low profile, enduring presence, minimal maintenance, and sizable areas of coverage, ADAS appears to be a natural system for covering unlikely (but still possible) enemy avenues of approach.

With Careful Placement, Acoustics Can Be Good "Cuer" for EFOG-M

- **Initial sensor placement resulted in few kills by EFOG-M**
  - **Majority of acoustic acquisitions were out of EFOG-M range**
  - **HIMARS response on acoustics were not played**
- **Minor adjustment to sensor laydown resulted in considerable increase of EFOG-M fires**
  - **127 launches**
  - **48 lost to air defense (2S6)**
  - **37 missed or reached end of tether and terminated**
  - **42 kills of which 2 were the intended (cueing) target**

ARROYO CENTER/NDRI RAND

The initial 21-sensor laydown that we received from DBBL needed to be modified somewhat for use with EFOG-M missiles. Because of the large distance of the EFOG-M launcher setback from the DRB front line, many of the ADAS target acquisitions from the original laydown were beyond the range of the missile. Taking the liberty to shift the 21-sensor laydown, by bringing the ADAS network in closer to the river (and the launchers), we were able to dramatically improve the contribution of the EFOG-M fires.

Our analysis shows that 12 EFOG-M launchers cued by ADAS resulted in a much higher number (127) of missiles being launched. Of these missiles, 48 were shot down by high-end tactical air defense units, the 2S6. Because many of the acquisitions were still near the maximum range of the missile, 37 either missed or reached the end of their tether before acquiring a target. The remaining 42 missiles successfully engaged and killed a target. It is interesting to note that only two of the targets that triggered a missile launch were ultimately among those killed by the missile. Most of the time, the missile locked on to another target in the area.[15]

[15]This appeared to be due to the large search area of the EFOG-M seeker and the density of targets in the engagement area. A more dispersed set of targets only partially reported by the acoustic sensors might have resulted in fewer launches and reduced weapon efficiency.

5. Observations

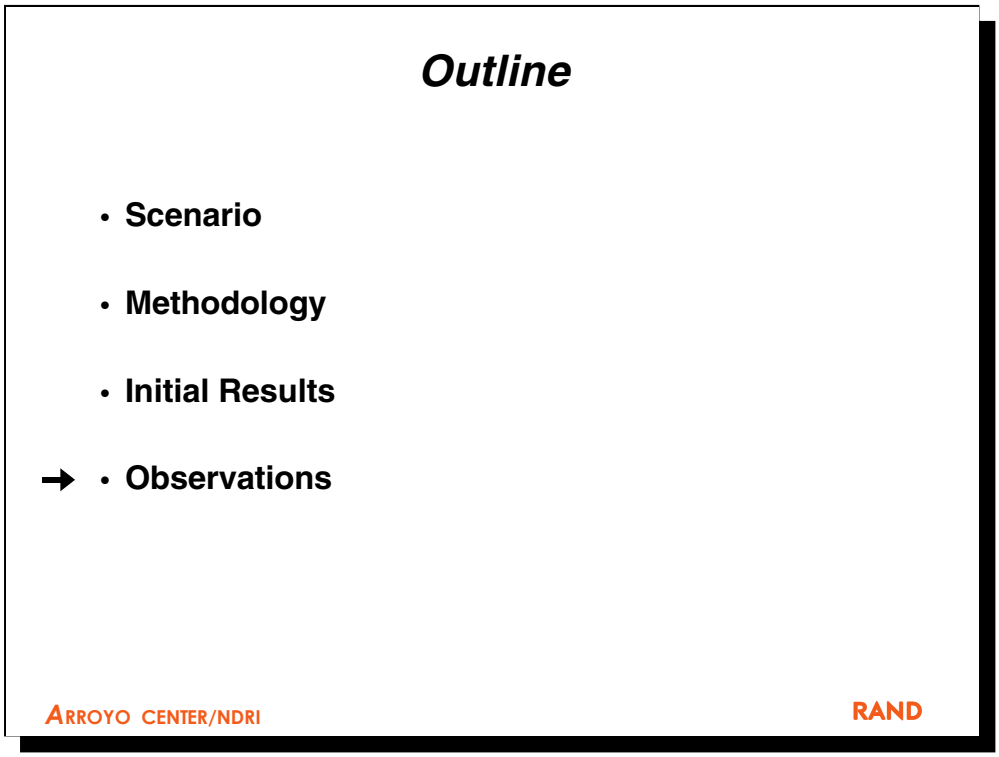

We conclude this report with a brief accounting of our key observations to date.

Preliminary Observations

- **Acoustic sensor network can provide wide range of information**
  - **Lack of completeness may require fusion with other sensors**
  - **Accuracy, while not up to expectations, was not a problem for large-footprint weapons**
- **Performance of acoustic sensors can be improved**
  - **Increasing numbers of sensors can improve on the completeness and accuracy of the information**
  - **Adjusting sensor spacings improved accuracy but reduced area coverage**
- **System integration needs to be defined**

ARROYO CENTER/NDRI RAND

Based on our analysis to date, we see acoustic sensor networks providing information across a broad spectrum, ranging from high-level situational awareness down to detailed targeting information. Nonetheless, we emphasize that these sensors come with inherent, unique limitations. Perhaps most critically, these sensors can become saturated fairly easily, resulting in incomplete representation of the target set. One solution to this was to increase the number of sensors used and place them closer together.

Another limitation of acoustic sensors, specifically the ADAS, was its larger-than-expected target location error. Used in conjunction with current-day weapons, this might be problematic. The limited accuracy of an acoustic sensor network can, however, be overcome if it is used in conjunction with a weapon system that has a sufficiently large footprint, like the EFOG-M.

As much analysis as has been performed, there needs to be much more focus on assessing ADAS as part of the RFPI system-of-systems. Questions about how best to use ADAS among other RSTA systems need to be addressed. We are taking steps in this direction and hope to provide more insights in the near future.

Appendix: ADVANCED ACOUSTIC SENSOR MODEL

A1. INTRODUCTION

This appendix describes an acoustic sensor network model that was developed as a part of RAND's work in support of the Rapid Force Projection Initiative (RFPI) Advanced Concept Technology Demonstration (ACTD). This model is intended to be applicable, with some modifications, to any type of acoustic ground sensor network. Its primary purpose, however, was to represent the performance of the air-deliverable acoustic sensor (ADAS), which is being built by Textron Systems Corporation for use in the field demonstration for this ACTD.

The specific intent of this appendix is to share our model with others in the defense simulation community. Therefore, the focus here is on the nature and architecture of the model itself, rather than on the phenomenology of the battlefield environment. Phenomenological issues were, however, investigated thoroughly, and the resulting insights were incorporated into the structure of the model and used to select appropriate values for input parameters. Simplifying assumptions were also made in three essential aspects of the model:

1. **Physical environment.** The ground is assumed to be flat, with no terrain features or vegetation.[1] Also, the meteorological and surface conditions used in this particular analysis only represent a single scenario: central Korea during the winter.[2]
2. **Ground vehicles.** All vehicles were assumed to be traveling at a constant speed of 30 kilometers per hour, and the acoustic emission spectrum of each vehicle was assumed to be fixed over time.

---

[1]The simulation does, however, include some information of this type, so a future version of the model could make use of it.

[2]A different scenario could easily be represented by using a different set of appropriate input data.

3. **Acoustic sensors.** The characteristics of the individual acoustic sensors are modeled on ADAS, which uses 0.5 Hz bins in the 50–250 Hz frequency range and uses conventional beamforming to make bearing estimates. These sensors were also assumed to be nonsaturating, so their performance is not degraded by high gain or local noise.

The remainder of the appendix is organized into three sections that describe the three levels of the modeling framework, shown in Figure A.1, and a final section that discusses acoustic location of artillery fires. Section A2 describes how the model generates the sound that each sensor hears. This includes the representation of acoustic sources, the propagation of sound from source to sensor, and the noise environment of the sensor. Section A3 explains how the model represents sensor performance in terms of array gain, detection, bearing estimation, and the resolution of sources. Section A4 describes the way the model fuses information from a network of acoustic sensors to provide target location estimates, and it also discusses the issue of target classification. Section A5 presents a standard method for locating artillery based on differences in the arrival times of firing events at different sensors.

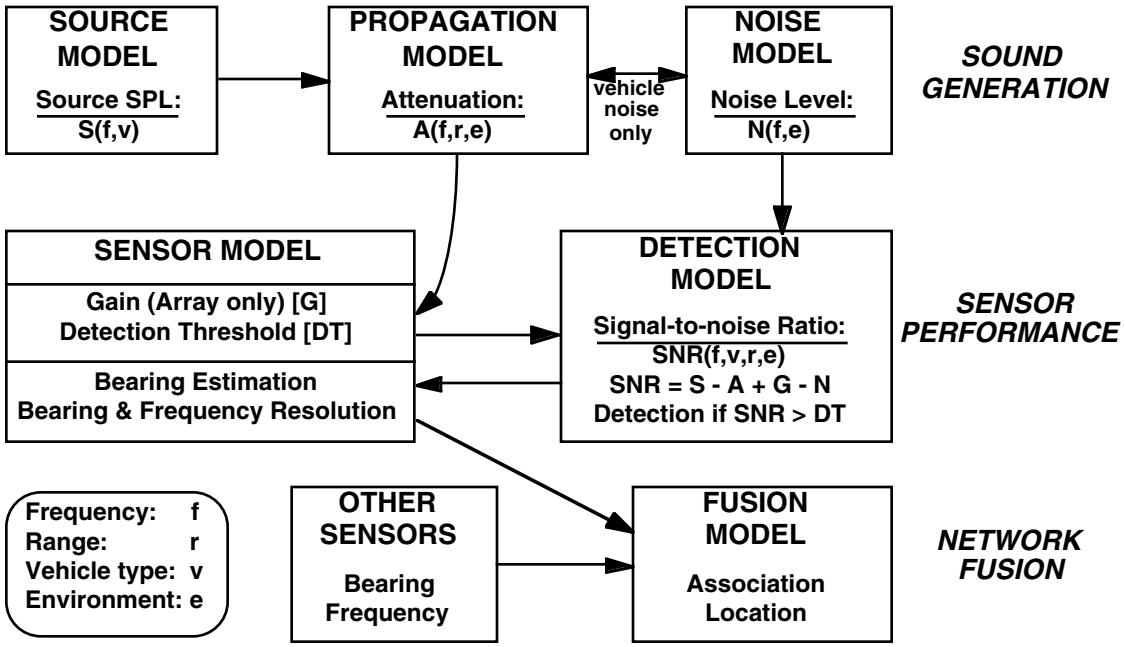

Figure A.1—Framework for Acoustic Sensor Network Model

A2. SOUND GENERATION

SIGNATURES OF ACOUSTIC SOURCES

There are two broad categories of acoustic source that can be represented in this sensor network model: ground vehicles and artillery firing events. It should be noted that although the model can accommodate both types of sound source, only the vehicle sources were actually implemented in the simulation. A notional representation of artillery firing events will be described briefly, but the primary focus of this section is on how the model handles vehicle sources.

Ground Vehicles

The spectral signature of a specific vehicle, indexed by i, is represented by a single "line," with a specific sound pressure level, or SPL, of L[i], and frequency of F[i], which is assigned to it at the start of a model run. The signature frequency F[i] is determined by drawing a frequency from a normal distribution with a mean (F*) and standard deviation (F_sd) specific to the vehicle's class or type, and then selecting the nearest 1/2 Hz frequency bin. For example, F[i] = 99.5 Hz if any frequency between 99.25 and 99.75 is drawn for vehicle i. L[i] is selected directly (i.e., without any bins) from a normal distribution with a mean of L* and a standard deviation of L_sd, which are again specific to that class of vehicles. Thus, there are four parameters that characterize the spectral signature distribution of a given class of vehicles: F*, F_sd, L*, and L_sd.

There are four vehicle classes in the model: heavy tracked, light tracked, heavy wheeled, and light wheeled. The values of the four parameters are shown in Table A.1 for each vehicle class. These parameter values were based on spectral data, provided by Textron Systems Corporation, for a representative vehicle type in each class.[3]

---

[3]The mean values are based on the largest peak in each spectrum. The standard deviations assume a standard deviation in engine firing rate of 100 rpm, taking into account engine specifications from Foss (1996).

Table A.1

Spectral Signature Parameter Values for Each Vehicle Class

Vehicle Class	Vehicle Type	F* (Hz)	F_sd (Hz)	L* (dB)	L_sd (dB)
Heavy tracked	T-72	115.5	2.50	118.3	1.5
Light tracked	BMP-2	92.5	1.25	119.2	1.5
Heavy wheeled	BTR-80	119.0	1.67	93.2	1.0
Light wheeled	HMMWV	79.5	1.67	100.9	1.0

The assigned frequency and SPL of each vehicle remain fixed over time during the simulation, even though the actual acoustic features of a moving vehicle are likely to vary considerably, since they are associated with the firing rate of the vehicle's engine. The underlying assumption here is that the spectral signature of a vehicle is essentially constant over the time intervals used for tracking (up to 30 seconds), and that each individual vehicle has a different mean signature. This assumption may not be strictly valid,[4] but it greatly simplifies the model and should not significantly affect the overall picture and insights that it provides. Of course, the appropriateness of this approach must ultimately be confirmed by comparing the model predictions to actual field test data.

Artillery Firing Events

Artillery launches are broadband impulse events, so there are no distinct spectral lines at specific frequencies. The ADAS will look for these events at low frequencies, in the range of 15 to 40 Hz, so the model could simply represent these events as a one-time interval pulse at 30 Hz. Two classes of artillery launch—cannon and rocket—should be considered, since acoustic characteristics of these two sources differ considerably. Both of these types of events are very loud, and cannon muzzle blasts vary somewhat more in loudness than rocket launches. These events could be represented in the model by a normal distribution in SPL with the parameters given in Table A.2. This approach would not, however,

[4]Movement of vehicles at nonuniform speeds will degrade the model's ability to discriminate targets and should require additional cues for identification, such as harmonics. Also, some complexities may arise with Doppler effects, which can change the frequencies by a few Hz for the vehicle speeds expected; but with most vehicles moving with similar velocities, these effects should be minimal.

Table A.2

Parameter Values for Artillery Firing Events

Artillery Class	Artillery Type	L* (dB)	L_sd (dB)
Cannon	155	175.0	6.0
Rocket	MLRS	185.0	3.0

permit the two types of firing events to be distinguished from each other, so some way of representing how the sensor tells them apart (rise times, spectral power distribution) would need to be developed and incorporated into the model to capture this capability.

ACOUSTIC PROPAGATION

The attenuation (A[i,k]) along the path from vehicle i to sensor k is determined using two look-up tables, one for the maximum attenuation and the other for the minimum. These tables were generated by a propagation model at the Pennsylvania State University Applied Research Laboratory (PSU-ARL).[5] Each table provides attenuation (in dB) at frequency intervals of 25 Hz from 25 Hz up to 250 Hz, and range intervals of 100 meters up to 10 kilometers.

For our analysis of a winter scenario in central Korea, we examined three cases: night, morning, and afternoon. A pair of attenuation tables was generated for each case, based on the typical meteorological conditions expected at that time of day, at a height of two meters above a frozen soil surface. These typical conditions, which are shown in Table A.3, are based on a ten-year average of weather station measurements at Chunchon, South Korea, provided by the Air Force Combat Climatology Center. It should be noted that these values only apply to the surface layer of the atmosphere, which is just a few meters thick. The conditions higher in the atmosphere are assumed to be quite similar in all three cases, converging at an altitude of 1,500 meters on a common wind speed (9 m/sec) and the typical adiabatic lapse rate (–10°C/km).

[5]Similar tables could, of course, be generated by any reliable propagation model. For a description and validation of this particular model, see Gilbert and Di (1993), and Swanson (1997).

Table A.3

Meteorological Conditions for the Three Scenario Cases

Case	Local Time	Temperature (°C)	Vertical Temperature Gradient (°C/km)	Wind Speed (m/sec)
Night	0:00	–5.8	+50	1.19
Morning	9:00	–8.0	–5	0.94
Afternoon	15:00	+0.1	–10	2.15

The very high positive temperature gradient (50°C/km) in the night case may at first seem unusual, but this value is indicative of a strong, but typical, temperature inversion near the surface. During the day, air near the ground is well mixed by wind and convection, so the temperature gradient near the surface is usually close to adiabatic. On a calm night, by contrast, a temperature inversion usually develops near the surface and inhibits mixing of the air nearest the ground, thereby reinforcing the positive temperature gradient. In such a situation it is not unusual for the temperature gradient to be as large as +50°/km, or +0.05°C/m in the first few meters of the atmosphere.

The attenuation on a given sensor-vehicle path is determined using a two-step process. First, the maximum and minimum attenuation ($A_{MAX}[i,k]$ and $A_{MIN}[i,k]$, respectively) are determined for the specific vehicle frequency (F[i]) and the sensor-vehicle range (R[i,k]) by interpolation, using attenuation tables. Next, the wind angle ($\alpha[i,k]$) is used to determine the total attenuation (A[i,k]) on that specific path. The attenuation is at its maximum when the wind is blowing from the sensor toward the source (due to upward refraction and shadow zone effects) and at its minimum when the wind is blowing from the source toward the sensor (due to downward refraction and reflection off the ground). The angle α, which can vary from –180° to 180°, is the difference between the bearing to the vehicle from the sensor and the bearing to the wind, as indicated in Figure A.2. The attenuation is calculated from α, $A_{MAX}[i,k]$, and $A_{MIN}[i,k]$ using the following elliptical interpolation:

$$A[i,k] = \frac{e \cdot p}{1 + e \cdot \cos\alpha}, \qquad (1)$$

where

$$e = \frac{A_{max} - A_{min}}{A_{max} + A_{min}},$$

$$p = \frac{2 \cdot A_{max} \cdot A_{min}}{A_{max} - A_{min}}$$

This approach assumes that wind speed and direction are constant along the path from the source to the sensor, and it only approximates the impact on attenuation of a cross wind. The propagation model used to generate the tables does, however, include the average effect on attenuation of wind turbulence near the ground (Gilbert and Di, 1993).

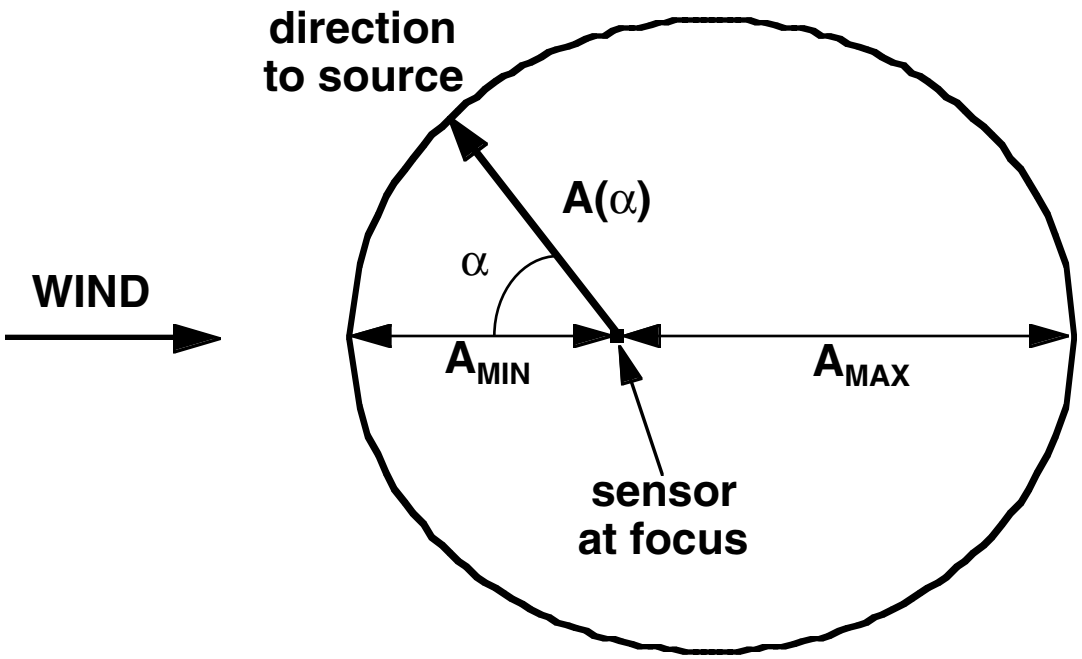

Figure A.2—Elliptical Interpolation Based on Wind Angle (α)

NOISE ENVIRONMENT

There are three potentially significant sources of noise for a ground-based acoustic sensor: ambient sounds, wind at microphones, and other vehicles. The noise associated with each of these sources will be calculated separately and then combined to obtain the total noise.

Ambient Noise

The ambient noise level at a given sensor (AN[i,k]) will be a function of an ambient noise parameter (AN_0), the frequency of the source it is searching for (F[i]), and an error term (AN_E[k]):

$$AN[i, k] = AN_0 + 20 \cdot \log_{10}(F[i]) + AN_E[k]. \tag{2}$$

The random error term AN_E[k] is normally distributed, with a mean of zero and a standard deviation of AN_sd. The two ambient noise parameters, AN_0 and AN_sd, will depend on the noise environment selected from the choices shown in Table A.4, which were provided by Textron Systems Corporation. This ambient noise model and the three noise environments are consistent with the acoustic specifications for the RFPI ACTD, as stated in Heberley (1995).

Table A.4

Ambient Noise Environment Parameters

Parameter	Units	Quiet	Nominal	Noise
AN_0	dB	56	64	76
AN_sd	dB	2	3	4

Wind Noise

The wind noise (WN[i,k]), which is caused by the wind blowing around the microphones of the sensor, is estimated as follows:

$$\begin{aligned} WN[i, k] = {} & WN_0 + WN_1 \cdot \log_{10}(F[i]) + WN_2 \cdot \log_{10}(WS) \\ & + WN_3 \cdot \log_{10}(WD), \end{aligned} \tag{3}$$

where WN_0, WN_1, WN_2, and WN_3 are wind noise parameters, WD is the windscreen diameter in centimeters, and WS is the wind speed at the microphones in meters per second (Strasberg, 1988). The wind noise parameters and the size of the windscreen are determined by the characteristics of the acoustic sensor microphones. The appropriate values for ADAS are given in Table A.5, and the wind speed for each of the three scenario cases is shown in Table A.3.

Table A.5

Wind Noise Parameters for ADAS Microphones

Parameter	Units	Value
WN_0	dB	76
WN_1	dB/log(Hz)	–25
WN_2	dB/log(m/sec)	63
WN_3	dB/log(cm)	–25
WD	cm	10

Vehicle Noise

In addition to ambient and wind noise, the model also estimates the local noise at each sensor that is due to the broad-band sound emissions of vehicles in its vicinity. It is assumed that each vehicle, indexed by j, generates a fixed level of background emissions at all frequencies other than its assigned peak frequency (F[j]). This background emission level is calculated by subtracting a background difference parameter, B_diff, from the peak SPL (L[j]) of each vehicle:

$$BL[j] = L[j] - B_diff. \quad (4)$$

The B_diff values used for each vehicle class are shown in Table A.6.[6]

[6]The value of B_diff was calculated for each vehicle class using the 25–250 Hz range of the corresponding sample spectra provided by Textron Systems Corporation.

Table A.6

Background Level Difference for Each Vehicle Class

Vehicle Class	Vehicle Type	B_diff (dB)
Heavy tracked	T-72	30
Light tracked	BMP-2	36
Heavy wheeled	BTR-80	26
Light wheeled	HMMWV	28

The contribution that each vehicle (j) makes to the local vehicle noise at a given sensor (k) when it is trying to detect a particular vehicle (i) is given by BN[i,j,k], which is calculated as follows:

$$BN[i,j,k] = BL[j,k] - BA[i,j,k] + G[i]. \tag{5}$$

In this expression, BA[i,j,k] is the attenuation along the path from vehicle j to sensor k (based on R[j,k] and α[j,k]) at the mean peak frequency (F*) of the class to which vehicle i belongs, and G[i] is the gain of the sensor at that frequency (see Section A3). The total vehicle noise at the sensor is VN[i,k], which is calculated as follows:

$$VN[i,k] = 10 \cdot \log_{10}\left(\sum_{j=1}^{M[k]} 10^{(BN[i,j,k]/10)} \right), \; j \neq i \,. \tag{6}$$

Here, M[k] is the total number of vehicles included in the local vehicle noise calculation, and the index j refers only to vehicles in a limited set of significant contributors.[7] The expression in equation (6) simply sums the received intensity levels associated with the background emissions of these vehicles to estimate their aggregate contribution to the local noise at the sensor (Kinsler et al., 1982).

[7]To reduce the number of calculations performed for each sensor, two approximations are used. First, the local vehicle noise contribution (BN[i,j,k]) is only calculated when the received signature SPL of the vehicle (j) is greater than the nonvehicle noise level (i.e., L[j] – A[j,k] > AN[j,k] + WN[j,k]). Second, the local vehicle noise at each sensor is only calculated once for each vehicle class, rather than being repeated for every vehicle.

Total Noise

Using the same approach, total noise at each sensor is calculated by adding the intensity levels of the noise from all three sources:

$$N[i,k] = 10 \cdot \log_{10}\left(10^{(AN[i,k]/10)} + 10^{(WN[i,k]/10)} + 10^{(VN[i,k]/10)}\right). \quad (7)$$

The nature of this calculation is such that the largest noise source dominates all the others. It is useful, however, to still include all three components because different sources will dominate under different circumstances.

A3. SENSOR PERFORMANCE

SENSOR GAIN

The gain of an acoustic sensor system depends on the nature of the sensor array, and how the system processes the information received by the array.[8] In the case of ADAS, which employs conventional beamforming, the total sensor gain is a nonlinear function of frequency. The model represented the gain of ADAS by interpolating between the values in a look-up table provided by Textron Systems Corporation.

DETECTION

For an acoustic sensor to detect the signature of a specific vehicle, the received signal of that vehicle must exceed the noise at that sensor by a certain detection threshold, which is a characteristic of the sensor system. For each vehicle-sensor path the signal-to-noise ratio (SNR) can be determined, given the SPL of the vehicle (L[i]), the attenuation along that path (A[i,k]), the gain of the sensor array (G[i]), and total noise level (N[i,k]) at the sensor, using the following simple calculation:

$$\mathrm{SNR}[i,k] = \mathrm{L}[i] - \mathrm{A}[i,k] + \mathrm{G}[i] - \mathrm{N}[i,k]. \tag{8}$$

Vehicle i will be detected by sensor k if the SNR[i,k] is greater than the detection threshold (DT) of the sensor (8 dB for ADAS).

Obviously, detection is a stochastic process, with the likelihood of detection increasing as the SNR increases. The model, however, assumes that detection is deterministic; a source is *always* detected if its SNR exceeds DT, and it is *never* detected if its SNR is below DT. This approach was taken because acoustic sensors are able to track the sources that they consistently detect over several seconds, while the time step of the simulation is considerably longer than this. In the model, if the source

[8]The term "sensor array" refers to an individual sensor system, as distinct from a "sensor network," which is a dispersed set of individual sensor arrays.

SNR is greater than the detection threshold, we assume the detection probability is high enough to maintain a track.[9] Thus, for this simulation, the detection of acoustic sources may be reasonably approximated using this deterministic approach.

BEARING ESTIMATION

The estimated bearing (B[i,k]) to vehicle i from sensor k is determined by adding two error terms to the actual bearing (B*[i,k]): a bias term (BE_b[k]) and a random error term (BE_r[i,k]):

$$B[i,k] = B^*[i,k] + BE_b[k] = BE_r[i,k]. \tag{9}$$

Bias is associated with environmental factors like wind and inherent calibration errors, while random errors are related to local noise. The total one-sigma error can be as high as 4° or 5° for sources that are barely detectable by the sensor.

Bias

The bearing bias (BE_b[k]) is assigned to each sensor from a normal distribution with a mean of zero and a standard deviation of B_bias. Once assigned, this bias remains fixed for each sensor throughout the simulation. The value of B_bias is determined from two uncorrelated sources of bias—calibration (B_cal) and environment (B_env):

$$B_bias = \sqrt{(B_cal)^2 + (B_env)^2}\ . \tag{10}$$

The value of B_cal for ADAS was provided by Textron, while the value of B_env is variable. It is difficult to reliably estimate an appropriate value for B_env, but it is reasonable to assume that it is correlated with wind speed and is usually on the order of 1° or 2°. Thus, in our analysis we used the values in Table A.7, but better estimates could be provided by field tests.

---

[9]Note also that we assume additive logarithmic effects in the model; that is, individual sensors do not saturate due to close noise sources or excessive gain settings.

Random Error

The random error component BE_r[i,k], on the other hand, is path dependent. It is assigned to each detection every time step from a zero-centered normal distribution with a standard deviation (B_ran[i,k]) that is a function of the vehicle frequency (F[i]), the received signal-to-noise ratio (SNR[i,k]), the number of elements in the array (m), the array radius (r), the speed of sound (c), the tracking filter time (t), and the frequency bandwidth (b) (Schultheiss, 1969):

$$B_ran[i,k] = \sqrt{\frac{\pi}{t \cdot b}} \cdot \frac{c}{2 \cdot r \cdot m} \cdot \left[\frac{(2\pi \cdot F[i])^2 \cdot 10^{(SNR[i,k]/10)}}{1 + M \cdot \sqrt{10^{(SNR[i,k]/10)}}} \right]^{-\frac{1}{2}}, \qquad (11)$$

where for ADAS m = 5, r = 0.61 m, b = 0.5 Hz, and t ≤ 30 sec. The speed of sound (c, in m/sec) is approximated by $c = 20 \cdot \sqrt{T + 273}$, where the temperature (T) is shown in Table A.3 for each case.

Table A.7

Environmental Bias Estimates for the Three Scenario Cases

Case	B_env
Night	1.0°
Morning	1.0°
Afternoon	2.0°

Comment on Artillery Firing Events

It should be noted that the approach described above is not appropriate for transitory artillery firing events. To estimate the location of such events, the time difference in the arrival of each impulse at the different sensors in the network would be calculated, taking into account the effect of a constant wind on the speed of sound propagation along a given path. Once detections of the same event by different sensors have been matched, then bearing estimates generated by pairs of sensors can be triangulated to determine the location of the source. (See Section A5 for a more detailed description of this process.)

RESOLUTION OF MULTIPLE SOURCES

An acoustic sensor may not be able to resolve all the acoustic signals it receives from multiple sources when those sources are close together in both frequency and bearing. There is an inherent limitation on a sensor's frequency resolution when the vehicle sources have similar spectral features. The signature features of vehicle spectra are typically only a few Hz in width, so if the signature features of two vehicles are too close together they will overlap and interfere with each other, making it impossible for a sensor to resolve the two signals. Acoustic sensors that employ conventional beamforming, as ADAS does, are also limited in bearing resolution by their small size.[10] When an ADAS receives signals from two similar sources with spectral features that overlap, it will be able to resolve them only if they are sufficiently separated in bearing for the beamformer to observe peaks at two different aspect angles. The exact resolution capabilities of an acoustic sensor are highly dependent on the details of its design. For ADAS, the bearing resolution was assumed to be 20°, since this is slightly less than half of its beam-steering interval of 45°. The frequency resolution of ADAS was assumed to be 3 Hz, based on the typical width of the signature features in the vehicle spectra.

The model represents these resolution difficulties by (1) generating bearing estimates for each detected vehicle, (2) checking each detection for a sufficient separation in either frequency or bearing to permit resolution, and (3) assigning each detection to a group of unresolved sources. Each group is treated as a single detection with the bearing and frequency of the loudest source in the group.[11] The bearings and frequency bins of the other group members are dropped, and thus they are not available for use in the process of associating detections and locating targets. Also, ADAS is assumed to only be able to track four detection groups at a time (based on its current software design). This group limit is important because it constrains the number of targets that the network as a whole can locate. For example, a cluster of three sensors, each with a group limit of four, can together locate no more than six sources.

---

[10]ADAS, like most advanced acoustic ground sensors, is designed for frequencies under 250 Hz, where vehicle emissions are the loudest, and the least attenuated. But at these frequencies the wavelength of the sound waves is comparable to the size of the sensor array, so the beamwidth is very large (about 45° at 3 dB for 250 Hz).

A4. NETWORK FUSION

ASSOCIATION AND LOCATION OF VEHICLE TARGETS

The first step in the network fusion process is to associate the bearing estimates made by different sensors. Since only one fundamental feature is assigned to each source, the frequency bin of this feature is used to match detections. The intersections of matched bearings then provide source location estimates. The model associates group detections by different sensors if they have the same frequency bin, and it considers them for triangulation to estimate the location of their potentially common source. Figure A.3 shows the location estimates that this process produced for a simple example of a three-sensor network. Each sensor has detected, resolved, and grouped the vehicles differently, so the frequencies of the bearings from each sensor are not identical. As a result, some bearings cannot be associated and fused, since no other sensor has centered a group on the same source.

---

[11]The group bearing could also be calculated as an SNR-weighted average of the bearings of all the members of the group.

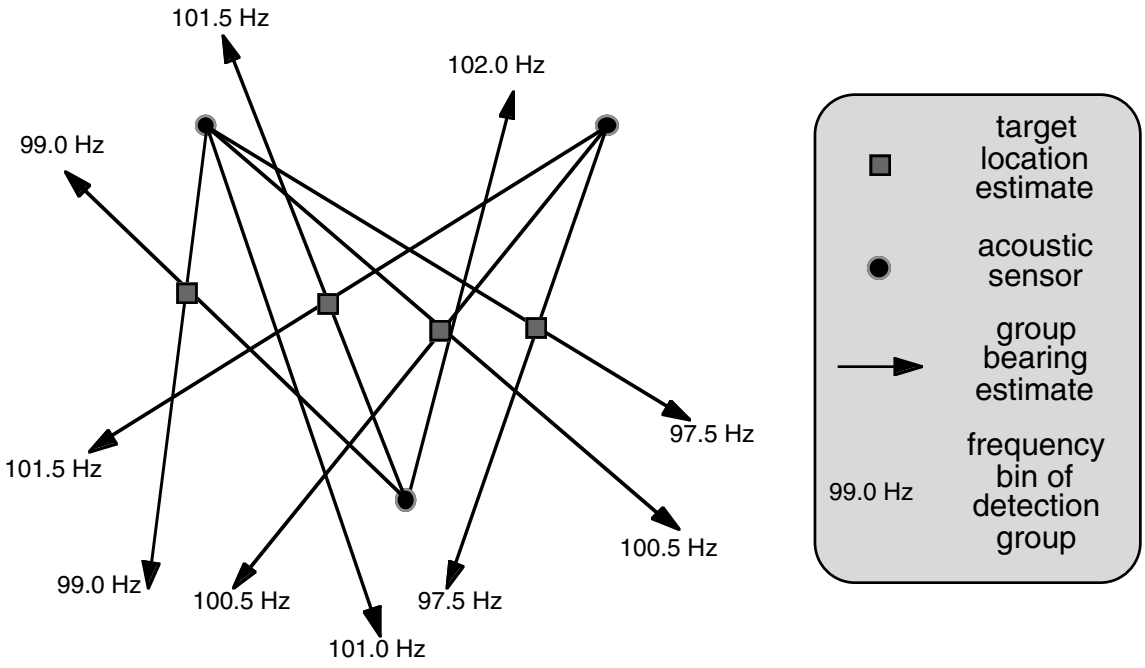

Figure A.3—Target Location by a Three-Sensor Network Using Triangulation

It is possible for more than one vehicle to be assigned to the same frequency bin, especially if the vehicles are of the same type, so there is always a chance that detections will be incorrectly associated, resulting in a false, or "ghost," target location. Many of these ghost targets can be eliminated by excluding potential triangulation points that are located beyond the expected sensor detection range. A ghost target in the upper right of Figure A.4 has been eliminated because it is beyond the expected detection range of one of the sensors being used to estimate its location.

Even if two detections are associated correctly, the location error can still be large if the bearing difference is close to 0° or 180°, due to the magnification of any small bearing estimation errors. The largest of these geometrically induced location errors are eliminated by applying a bearing difference limit (BDL) to the matched bearing pairs. Potential triangulation points are eliminated if the difference between the two bearing estimates is less than BDL or greater than 180 – BDL, where BDL

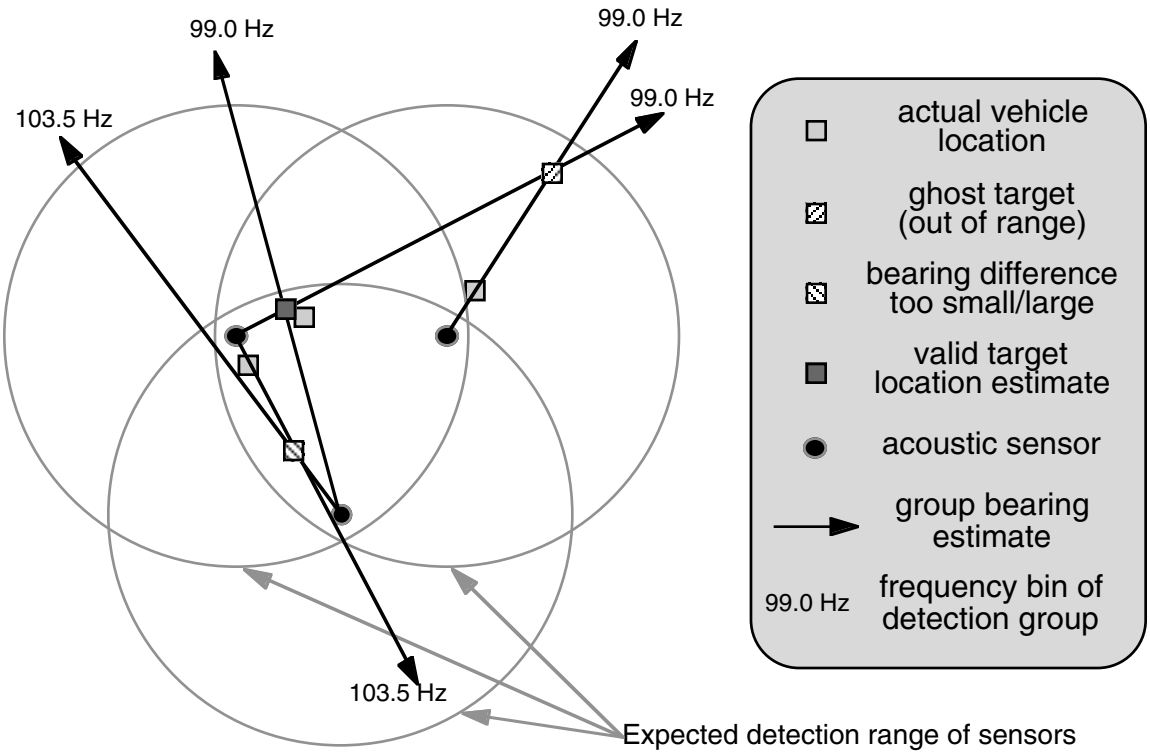

Figure A.4—Elimination of Potential Triangulation Points to Avoid Ghost Targets and Reduce Geometrical Location Errors

is the minimum angle permitted between the two intersecting bearing lines.[12] A potential triangulation point in the upper left of Figure A.4 has been eliminated for this reason. In addition, when multiple pairs of matched bearings are available, the pair with the bearing difference closest to 90° is used to estimate location, since its geometric triangulation error is likely to be the smallest.

It is also possible to estimate the location of a vehicle when only one sensor has detected it, provided we assume that (1) the vehicle is traveling on a road and (2) the sensor knows its own location and has an accurate road map. In this case, the point where the estimated bearing from the sensor to the detected source crosses a road can be used as a location estimate. Figure A.5 illustrates how this approach works with a simple straight road and a network of three sensors. Of course, the bearing line

[12]A reasonable range for BDL is 5° to 35°; a lower value indicates a greater tolerance for geometric errors.

may cross a more complex road system more than once, so in implementing this approach the model applies some simple rules to pick the best crossing point. First, any crossing points that are beyond the expected detection range of the sensor are eliminated. Second, any points where the bearing crosses the road at an angle of less than 10° are eliminated, since these points are sensitive to small bearing errors. The remaining crossing points are evaluated, and one is selected as the "best" location estimate. In its "road fusion" mode, the model can merge road crossing point data from the entire sensor network to select the "best" target location estimates, and it can even form a "blob," or line, of adjacent vehicles along a road.

LOCATION OF ARTILLERY SOURCES

Differences in the arrival time at different sensors of distinctive sounds associated with an artillery firing event can be used to locate its source. Section A5 describes in some detail a method for using acoustic sensors to determine the location of artillery, which is based on a conventional sound ranging technique (Innes, 1950). This approach was never actually implemented in our acoustic sensor network model, but it could be added without much difficulty.

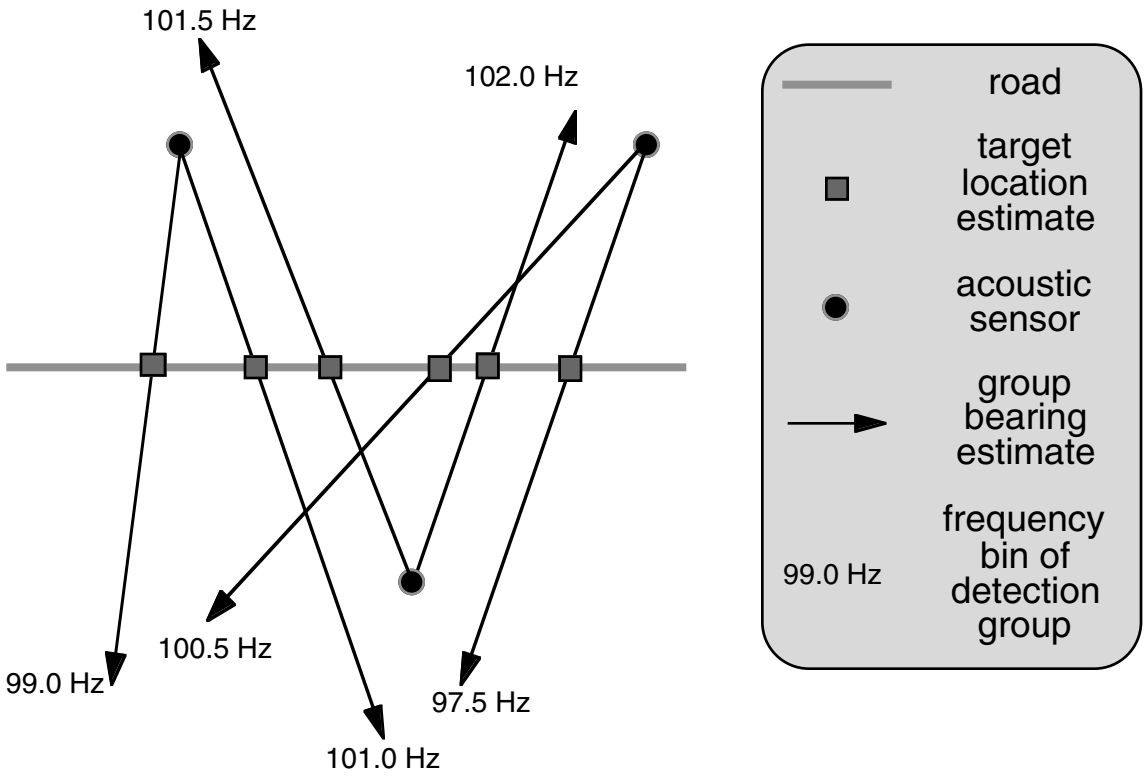

Figure A.5—Target Location by a Three-Sensor Network Using Road Fusion

TARGET CLASSIFICATION CONSIDERATIONS

Networks of advanced acoustic sensors, such as ADAS, may be able to use spectral information to classify the vehicle and artillery targets they detect and locate. This model, however, cannot incorporate the classification process because its simple representations of vehicle source spectra are inadequate for this task. In addition, even if a more sophisticated representation of the sources were used, it would still be difficult to accurately capture the classification performance of real sensors in a simple manner, without implementing the actual classification algorithms used by the sensor. These classification schemes may be unavailable, and even if they are they are likely to be too cumbersome to be integrated easily and efficiently into a large-scale simulation. An attractive alternative might be to assign classifications using probabilities from a

confusion matrix based on field test data for the sensor under consideration. If comprehensive field data are not readily available, a computer simulation could be used to produce statistics over a wide range of assumptions. Environmental, target, and background data could be collected, input to a sensor model, and used to generate simulated observables, which could then be processed by the classifier to generate the necessary confusion matrix.

A5. METHOD FOR LOCATING ARTILLERY FIRING EVENTS

This section presents a method for using acoustic sensors to determine the location of artillery. This method (Innes, 1950) is essentially the same as the sound ranging technique that was used to locate artillery on the battlefield during World Wars I and II and other 20th century conflicts. The method assumes that each artillery event is distinguishable in time or signature.

ARRIVAL TIME DIFFERENCE

The only source of location error that this technique takes into account is wind. It is assumed that the time measurement and coordination errors are negligible. Temperature (T), wind speed (WS), and wind direction are assumed to be constant in space and time, and the sensor system is assumed to know the temperature but not the wind speed or direction. The base sound speed is given by $c = 20 \cdot \sqrt{T + 273}$, where the temperature (T) is shown for each case in Table A.3. The sound speed along a path from artillery event p to sensor k is given by

$$SS[p,k] = c + WS \cdot \cos(\alpha[p,k]), \tag{12}$$

where $\alpha[p,k]$ is the angle between the direction the wind is blowing from and the bearing from sensor k to artillery firing event p.

The time taken for the sound of artillery event p to travel to sensor k is given by

$$TT[p,k] = R[p,k] \,/\, SS[p,k], \tag{13}$$

where R[p,k] is the range of artillery firing event p from sensor k. The difference in the arrival time of artillery event p at a pair of sensors, indexed by k and q, is given by:

$$TD[p,k,q] = TT[p,q] - TT[p,k]. \tag{14}$$

The equivalent delay distance is then given by

$$DD[p,k,q] = c \cdot TD[p,k,q] + Normal\left(DD_sd[p,k,q]\right), \tag{15}$$

where DD_sd[p,k,q] is the standard deviation of the normally distributed error in the measurement of the delay distance by the pair of sensors, given by the following expression:

$$DD_sd[p,k,q] = c \cdot SS_fsd \cdot WS \cdot \sqrt{\left(\frac{R[p,k]}{SS[p,k]^2}\right)^2 + \left(\frac{R[p,q]}{SS[p,q]^2}\right)^2}, \tag{16}$$

where SS_fsd is the standard deviation of the sound speed along the path from the source to the sensor, as a fraction of the wind speed (WS).

SOURCE LOCATION

The baseline distance between this pair of sensors is BL_D[k,q], with a midpoint located at (BL_X[k,q], BL_Y[k,q]), and a bearing from sensor k to sensor q of BL_B[k,q]. The arrival time difference between each pair of sensors generates a hyperbola that is the locus of all of the points where the delay distance is equal to the difference in the distance from the source to the two sensors. In the reference frame of the baseline (X,Y), with the midpoint as the center and the sensors at the foci, the hyperbola is expressed as

$$\frac{X^2}{DD[p,k,q]^2} - \frac{Y^2}{BL_D[k,q]^2 - DD[p,k,q]^2} = \frac{1}{4}. \tag{17}$$

This hyperbola must then be rotated to the bearing of the sensor pair baseline, BL_B[k,q], and translated to the midpoint of that baseline, (BL_X[k,q], BL_Y[k,q]), using the following transformation:

$$\begin{aligned} x &= BL_X[k,q] + X \cdot \cos\left(BL_B[k,q]\right) - Y \cdot \sin\left(BL_B[k,q]\right) \\ y &= BL_Y[k,q] + X \cdot \sin\left(BL_B[k,q]\right) + Y \cdot \cos\left(BL_B[k,q]\right). \end{aligned} \tag{18}$$

Any two hyperbolas can be used to estimate the location of the artillery firing event by finding the point where they intersect. Hyperbolas associated with pairs of sensors that have a bearing difference outside of the usual limits (i.e., below BDL or above 180 – BDL) are eliminated to reduce potentially large geometric errors. There are two options for how the remaining hyperbolas can be used to estimate the location of the firing event: (1) pick the "best" two and find their intersection point or (2) pick the "best" three, find the three intersection points, and determine the centroid.

ITERATIVE APPROXIMATION

A quick alternative to finding the intersection of the two hyperbolas is to use their asymptotes instead. This is less accurate than using the actual hyperbolas, but it works quite well when the source is more than 3 or 4 kilometers away from the sensors and the actual bearings from the midpoints of the sensor pair baselines are not too close together. The angle of asymptote (θ) is measured clockwise from the perpendicular bisector of the baseline, and it is calculated using

$$\sin\theta = DD[p,k,q] \,/\, BL_D[k,q]. \tag{19}$$

It should be noted that both values of θ that satisfy this equation are possible, as the source could be on either "end" of the hyperbola, with the appropriate branch of the hyperbola determined by the sign of DD[p,k,q].

The intersection point of the asymptotes from two different baselines provides an estimate of the source location. The distance to this location from the baseline midpoint ER[p,k,q] is used to correct the time delay TD[p,k,q] by

$$\Delta TD[p,k,q] = TD[p,k,q] \cdot \left(\sqrt{1 + \frac{c^2 \cdot \left(BL_D[k,q]^2 + TD[p,k,q]^2 \right)}{4 \cdot ER[p,k,q]^2}} - 1 \right). \tag{20}$$

After this correction is made, new bearings are calculated for each of the two sensor baselines and then used to generate a new, more accurate

location estimate. One or two iterations of this type should be sufficient to eliminate most of the error.

APPENDIX SOURCES

Burdic, W. S., *Underwater Acoustic System Analysis*, 2d ed., Englewood Cliffs, NJ: PTR Prentice Hall, 1991.

Foss, C. F. (ed.), *Jane's Armour and Artillery: 1996–97*, Coulsden, Surrey, U.K.: Jane's Information Group, 1996.

Gilbert, K. E., and X. Di, "A Fast Green's Function Method for One-Way Sound Propagation in the Atmosphere," *Journal of the Acoustical Society of America*, Vol. 94, No. 4, 1993, pp. 2343–2352,.

Heberley, Jeff, *Acoustic Sensor (AOS) Specification for RFPI*, Picatinny, NJ: United States Army Armament Research, Development and Engineering Center, May 1995.

Innes, F. T., *Sound Ranging for the Field Artillery*, Philadelphia, PA: The Franklin Institute Laboratories for Research and Development, Technical Memorandum, ORO-T-62, 15 January 1950.

Kinsler, L. E., A. E. Frey, A. B. Coppens, and J. V. Sanders, *Fundamentals of Acoustics*, 3d ed., New York: John Wiley & Sons, 1982.

Schultheiss, P. M., "Optimum Passive Bearing Estimation in a Spatially Incoherent Noise Environment," *Journal of the Acoustical Society of America*, Vol. 46, No. 1, 1969, pp. 37–43.

Strasberg, M., "Dimensional Analysis of Windscreen Noise," *Journal of the Acoustical Society of America*, Vol. 83, No. 2, 1988, pp. 544–548.

Swanson, D. C., "Acoustic Detection Validation in a Desert Environment," *The Fifth Battlefield Acoustics Symposium, Conference Proceedings*, Fort Meade, MD, 23–25 September 1997, pp. 69–89.

BIBLIOGRAPHY

Boatman, J., M. Hammick, and B. Sauerwein, "The Future of Armored Recce," *International Defense Review*, October 1992, pp. 965–973.

Bonsignore, E., "Russian Gun-Launched Anti-Tank Missiles," *Military Technology,* July 1993, pp. 64–68.

Cassidy, J. F., *Transportability for Better Strategic Mobility: A Guide to Engineering for Transportability*, Military Traffic Management Command, Transportation Engineering Agency (MTMCTEA) Pamphlet 70-1, 1987.

Combat Engineer Systems Handbook, Fort Leonard Wood, MO: U.S. Army Engineer School, April 1991.

Flynn, K. S., and J. Miller, "Hunter-Killer Operations," *Armor*, July–August 1993, pp. 48–50.

Force XXI Operations, TRADOC Pamphlet 525-5, 1994.

Goodman, G. W., "Army's Javelin Antitank Weapon: 'Fire and Forget' Past Problems," *Armed Forces Journal International,* October 1992, pp. 14–15.

Gourley, S. R., "Fighting with Fires: US Artillery Modernization," *Military Technology*, December 1994, pp. 8–14.

Grimes, V. P., "U.S. Army Begins Digitization Build-Up," *International Defense Review*, August 1994, pp. 51–54.

Hewish, M., and R. Pengelley, "Acoustics on the Battlefield," *Defense Electronics and Computing (Supplement to IDR 4/1990),* pp. 47–49.

Matsumura, J., R. Steeb, T. Herbert, S. Eisenhard, M. Lees, and A. Stich, *Analytic Support to the Defense Science Board: Tactics and Technology for 21st Century Military Superiority,* Santa Monica, CA: RAND, DB-198-A, 1997.

Ogorkiewicz, R. M., *Technology of Tanks,* vols. 1 and 2, Coulsdon, Surrey, UK: Jane's Information Group, 1991.

Pengelley, R., "Tank Ammunition Development," *International Defense Review*, April 1994, pp. 39–46.

Robinson, C. A., "Army Charges Toward Future: Seizing Technology's Strength," *Signal,* May 1995, pp. 79–85.

———, "Geospatial Information Pinch Creates Digital Balancing Act," *Signal*, November 1995, pp. 45–49.

Steeb, R., K. Brendley, T. Covington, T. Herbert, and D. Norton, *Light Forces—Heavy Responsibilities: The Role of Technology in Enabling Future U.S. Early Entry Forces to Fight and Survive,* Santa Monica, CA: RAND, MR-473-ARPA, 1995.

Stix, G., "Fighting Future Wars," *Scientific American*, December 1995, pp. 92–98.

Sullivan, GEN G., and LTC J. Dubic, *Land Warfare in the 21st Century*, U.S. Army War College Fourth Annual Conference on Strategy, February 1993.

"TOW: An Example of Continuous Upgrade," *National Defense*, February 1991, pp. 30–33.

Womack, S., "The AGS in Low-Intensity Conflict: Flexibility Is the Key to Victory," *Armor*, March–April 1994, pp. 42–44.

"U.S. Army to Demonstrate Fiber-Optic Missile and Guided Mortars," *International Defense Review*, June 1994, p. 13.